

1 **Head and Neck Response of an Active**
2 **Human Body Model and Finite Element**
3 **Anthropometric Test Device During a**
4 **Linear Impactor Helmet Test**

5
6 **David A. Bruneau**

7 Department of Mechanical and Mechatronics Engineering, University of Waterloo
8 University of Waterloo, 200 University Ave. West, Waterloo, Ontario, Canada, N2L 3G1
9 dbruneau@uwaterloo.ca

10
11 **Duane S. Cronin¹**

12 Department of Mechanical and Mechatronics Engineering, University of Waterloo
13 University of Waterloo, 200 University Ave. West, Waterloo, Ontario, Canada, N2L 3G1
14 duane.cronin@uwaterloo.ca

15
16 **Acknowledgments:** The research presented in this paper was made possible by a grant
17 from Football Research, Inc. (FRI). The views expressed are solely those of the authors
18 and do not represent those of FRI or any of its affiliates or funding sources.
19

¹ Department of Mechanical Engineering, University of Waterloo, 200 University Ave. West,
Waterloo, Ontario, Canada, N2L 3G1, dscronin@uwaterloo.ca, (519) 888-4567 x32682.

1 **ABSTRACT**

2 *It has been proposed that neck muscle activation may play a role in head response resulting from*
3 *impacts in American Football. The importance of neck stiffness and active musculature in the standard*
4 *Linear Impactor Helmet Test was assessed using a detailed head and neck finite element (FE) model from a*
5 *current Human Body Model (HBM) compared to a validated Hybrid III head and neck FE model. The models*
6 *were assessed for bare-head and helmeted impacts at three speeds (5.5, 7.4, 9.3 m/s) and three impact*
7 *orientations. The HBM head and neck was assessed without muscle activation, and with a high level of*
8 *muscle activation representing a braced condition. The HBM and Hybrid III had an average cross-*
9 *correlation rating of 0.89 for acceleration in the primary impact direction, indicating excellent*
10 *correspondence regardless of muscle activation. Differences were identified in the axial head acceleration,*
11 *attributed to axial neck stiffness (correlation rating of 0.45), but did not have a large effect on the overall*
12 *head response using existing head response metrics (HIC, BrIC, HIP). Although responses that develop over*
13 *longer durations following the impact differed slightly, such as the moment at the base of the neck, this*
14 *occurred later in time and therefore did not considerably affect the short-term head kinematics in the*
15 *primary impact direction. Though muscle activation did not play a strong role in the head response for the*
16 *test configurations considered, muscle activation may play a role in longer duration events.*

17

1 INTRODUCTION AND BACKGROUND

2 Football helmets have reduced the risk for Traumatic Brain Injury [1] and an
3 ongoing challenge is to continue reducing the risk for Mild Traumatic Brain injury (mTBI)
4 through improved helmet design. Helmet performance is assessed experimentally using
5 the National Operating Committee on Standards for Athletic Equipment (NOCSAE) Drop
6 Test [2], and more recently, the linear impactor test incorporating an existing
7 Anthropomorphic Test Device (ATD) headform and neck, which has been used to evaluate
8 helmets in academic studies [2–4]. The linear impactor test will be used by NOCSAE to
9 certify helmets as of May 2019 [5]. There is currently no representation of active
10 musculature in the ATD neck, and it has been suggested that the higher stiffness of the
11 ATD neck and lack of active musculature may contribute to the measured response [4,6].

12 The linear impactor test incorporates the head and neck from a Hybrid III 50th
13 percentile male ATD mounted on a sliding carriage, which is free to translate in the same
14 direction as the impactor (See Supplemental Materials, Figure S1). The carriage, head and
15 neck has a combined mass of 23.1 kg, while the impactor has a mass of 15.4 kg, which
16 represent a player’s kinematic properties during an impact to the head [3,4,7]. The Hybrid
17 III head is made of aluminum with a mass of 4.54 kg and covered in a vinyl skin with
18 internally mounted accelerometers to record the kinematics. The Hybrid III neck is a
19 passive structure consisting of rubber and metal discs, which allows for rotation of the
20 head. Incorporation of the neck is intended to produce a more biofidelic head response
21 compared to the NOCSAE drop test, where the headform is fully constrained to the test

1 apparatus. In the linear impactor test, the helmet, donned on the head is impacted with
2 a linear impactor at a specific velocity and impact location. The impactor has a nylon end
3 cap and a vinyl-nitrile foam pad which represent an incoming helmeted head [2,8]. From
4 both tests, NOCSAE assesses the head kinematics using the Severity Index (SI), which is
5 calculated from the resultant linear head acceleration [8]. However, many different
6 kinematic criteria have been investigated to assess head kinematics from the Hybrid III
7 [9–11], as well as brain deformation from a finite element model driven by the kinematics
8 of the Hybrid III [4,6,8]. Despite the widespread use of the Hybrid III in assessing football
9 helmet impacts, how the head kinematics compare to those of a more biofidelic human
10 model is still not well understood [12,13], and the role that muscle activity plays in these
11 impacts is also not well understood [14]. Some studies have shown that the Hybrid III neck
12 is stiffer than a cadaveric human neck [13] in axial compression, while others have
13 suggested that the Hybrid III neck is not stiff enough [2] for football impact testing. The
14 Hybrid III was designed for anterior-posterior loading, while the linear impactor test
15 comprises of loading in multiple directions [15], leading to lateral neck loading, axial
16 rotation, and often combined modes of loading. The biofidelity of the Hybrid III is
17 frequently cited as a limitation of studies which use it to predict head kinematics
18 [4,15,16].

19 In addition to studies which use an isolated head model driven by experimental
20 kinematics, some recent studies have integrated finite element models of football
21 helmets with detailed Human Body Models (HBM) [14,17,18]. These HBMs have a high

1 level of detail in biomechanical structures when compared to ATDs, and provide an
2 opportunity to investigate the effect of muscle activation. However, no previous studies
3 have compared the performance of the HBM to that of an ATD. In previous studies of
4 football impacts which have simulated the relevant neck structures with HBMs [14,18],
5 the Global Human Body Models Consortium (GHBMC [19]) 50th percentile male model has
6 been used. However, in these studies the helmet models were limited by a small number
7 of validation cases, little to no material testing, and the use of material models which did
8 not capture the important effects of viscoelasticity exhibited by many currently used
9 helmet materials. Further, previous models lacked detail in the areas of the chin strap and
10 facemask, which are necessary to properly capture football helmet impacts in some
11 orientations [20,21]. Johnson [17] considered facemask impacts in a linear impactor
12 scenario with a football helmet model developed from measured material properties,
13 with the purpose of optimizing facemask design using brain response. However, this
14 helmet model was not validated at the full helmet level, and there was no mention of
15 how the head model was constrained in the simulations as there was no neck included in
16 the study. One impact speed of 6 m/s was considered, which is not typically associated
17 with concussive impacts [8]. Darling [18] used the GHBMC full body model fitted with a
18 simplified football helmet model to investigate regional brain strains in frontal and crown
19 impacts with a rigid impactor. The football helmet model consisted of a low-density foam,
20 a high density foam and a polycarbonate shell, and was validated using a single drop test.

1 The model lacked a face mask and chin strap, and neck stiffness or active musculature
2 were not investigated.

3 Some studies have examined the effect of neck musculature in a football helmet
4 impact [14,22,23]. The majority have focused on human subjects and have not measured
5 muscle activity at the time of impact. In football helmet impacts, the impact is transmitted
6 directly to the head, in contrast with the more prevalent studies concerning car crashes
7 where the impact is translated from the body to the head. In car crash scenarios, active
8 musculature has been shown to have a significant effect on the head kinematics [24].
9 Experimentally, Eckner et al. [23] observed a correlation between anticipatory muscle
10 activity and decreased head angular velocity in a test on human participants, using non-
11 injurious impulses directly to the head (resultant angular velocity of 2 – 3.5 rad/). A braced
12 and relaxed condition were tested, with the braced condition exhibiting 15% lower
13 angular velocity.

14 The GHBMC neck model has been used to investigate the influence of active
15 musculature on head and neck response in car crash scenarios [24]. However, only one
16 study of football helmet impact to a HBM has considered the effect of active musculature
17 [14]. Muscles in the GHBMC neck model are modeled using solid 3D elements for the
18 passive properties and 1D axial elements for the active properties, which are attached to
19 the 3D elements at small increments to allow a biofidelic line of action [19,25]. The 3D
20 solid elements are modeled using a hyperelastic Ogden function while the 1D axial
21 elements use a Hill-type muscle element [26]. The muscles in the GHBMC neck model are

1 classified as flexors, which rotate the head forwards, and extensors, which rotate the
2 head backwards (See Supplemental Materials, Table S5 for all muscles included in the
3 model). The flexor and extensor muscles are activated separately using a dimensionless
4 Activation Level (AL) as a function of time [14,24]. Jin et al. [14] studied the effect of
5 muscle activation during football helmet impacts using the GHBMC head and neck model,
6 with part of the torso included. This study suggested that early activation of musculature
7 reduced the angular velocity of the head. A single lateral impact at a speed of 9.5 m/s was
8 simulated, based on an impact reconstruction which used two Hybrid III ATDs. The exact
9 positioning of the ATDs and helmet in the reconstruction was unknown, so the HBM was
10 positioned by guessing the head position, then adjusting the position so that the
11 translational acceleration traces of the HBM head and the ATD matched as closely as
12 possible. This study used a model of a Riddell VSR4 helmet, validated in 4 cases at a speed
13 of 7 m/s and developed using Computed Tomography (CT) scans. This helmet model
14 included a chin strap with no pre-tension and a face mask. The material properties were
15 not all measured from samples of the components, but mostly prescribed from
16 manufacturer obtained properties. The foam material model used a single stress-strain
17 curve determined at an unspecified rate and it was unclear if viscoelasticity was included
18 in the model. Four muscle activation schemes were used, and with muscle activation prior
19 to impact, a 20% decrease in peak rotational velocity was observed. In this study, the
20 flexor and extensor muscles were given the same muscle activation curve, which causes
21 the GHBMC head to rotate quickly backwards due to higher forces generated by the

1 extensor muscles. Since the impact timing in this study varied, the changes in head
2 response observed in this study that were attributed to active musculature could have
3 been caused by the head moving into a different position prior to impact. While this study
4 was a promising investigation of the effect of active musculature, it would be beneficial
5 to investigate the effect of impact orientation and speed, while using a football helmet
6 model with more experimental validation and known positioning of the ATD, HBM and
7 helmet at the time of impact.

8 Recently, a large dataset of linear impactor experiments using four modern
9 football helmets were conducted by Biocore, LLC using a 50th percentile Hybrid III ATD
10 head and neck [27,28]. Four helmets, including the 2016 Xenith X2E football helmet
11 (Safety Equipment Institute model X2E), were tested in eight standard impact
12 orientations, at 3 different speeds ranging from regular gameplay (5.5 m/s) to speeds that
13 potentially cause concussion (7.4 and 9.3 m/s) [3,8]. In addition to the experiments, four
14 finite element models of the same football helmets were developed, validated against
15 the experiments, and made publically available. The helmet model response was
16 compared to the measured experimental response using cross-correlation (Correlation
17 and Analysis (CORA) software, PDB, Germany), which compares two transient response
18 signals using signal magnitude, shape and phase shift [28–30]. The outcome is a rating
19 between 0 (poor correlation) and 1 (excellent correlation). CORA has been used in many
20 biomechanics publications and provides a detailed, objective indication of simulation
21 quality [28,29,31,32].

1 The first objective of the current study was to compare the head kinematics of a
2 detailed HBM head and neck FE model to those of the Hybrid III ATD head and neck FE
3 model using the boundary conditions of the linear impactor test. The effect of impact
4 orientation and speed were examined for bare-head and helmeted impact scenarios. A
5 secondary objective was to investigate the effect of active neck musculature in the HBM,
6 by comparing a high level of muscle activation and no muscle activation in the HBM. It
7 was hypothesized that the higher neck stiffness of the ATD compared to the HBM would
8 affect head kinematics at long durations following the impact, but would not affect short-
9 term head kinematics associated with current assessment criteria.

10

11

1 **METHODS**

2 A deformable linear impactor FE model (Figure 1a) [7] was used to impact using
3 two existing FE models of the head and neck: a 50th percentile male Hybrid III ATD (Figure
4 1b) and the 50th percentile male GHBM HBM (Figure 1c). Helmeted impacts were
5 simulated using the Xenith X2e Helmet Model (Figure 1d), as well as bare-head impacts.
6 All FE models were analyzed using a commercial explicit FE code (LS-DYNA R7.1.2, LSTC,
7 Livermore, California).

8 **Boundary Conditions**

9 The base of the neck of the ATD and the linear impactor were constrained (Figure
10 2) so that only translation in the global X direction (Figure 2) could occur, with no rotation
11 permitted. For the HBM, the first thoracic vertebrae (T1) was constrained to only allow
12 for translation in the global X direction. No other boundary conditions were applied to
13 the models. In the current study, three impact directions denoted as “F” (frontal), “C”
14 (coronal or lateral), and “R” (rear) were investigated (Figure 3), which corresponded with
15 three of the impact orientations used in physical helmet testing [3,8], and for which the
16 helmet FE model was validated with the ATD model [27]. Some studies have suggested
17 that the head has a lower injury threshold in a coronal plane impact compared to a sagittal
18 plane impact [33,34], while others have shown that frontal impacts are the most common
19 head impact location in gameplay [35]. Importantly, the three impact orientations were
20 approximately 90° apart, which flexed the neck in the lateral, anterior and posterior

1 directions. These orientations induced motion primarily in one plane, to clearly
2 understand the effect of active musculature on the resulting head kinematics in the
3 sagittal and coronal planes (an example of the out-of-plane motion is included in the
4 Supplemental Materials, Figure S6 and Figure S7). Three impact speeds of 5.5 m/s, 7.4
5 m/s and 9.3 m/s were used for all simulations (Figure 3), corresponding to impact speeds
6 from the experimental data. Bare-head cases were simulated as well as helmeted cases
7 (Figure 3).

8 **Existing Models**

9 *Impactor Finite Element Model*

10 The FE model of the deformable impactor (the construction of which was
11 previously detailed in [7,28]) (Figure 1a) used a hyperelastic, viscoelastic model for the
12 foam, and an elastic material for the nylon end cap [28]. The foam material was developed
13 from experiments over a range of 8 tested rates, and the impactor model was previously
14 validated against three dynamic compression experiments [28]. The total mass of the
15 linear impactor model was the same value specified in the NFL helmet test protocol (15.4
16 kg) [7].

17 *Anthropometric Testing Device Finite Element Model*

18 The ATD model used in the current study was a previously developed FE model of
19 the head and neck of a 50th percentile male Hybrid III ATD [28] (Figure 1b). The ATD and
20 impactor models were previously validated together [28], and verified against the

1 reported experimental impact response as the first step of the current study, with an
2 average overall CORA rating of 0.79 (Supplemental Materials, Table S6 and S7).

3 *Human Body Model*

4 The Human Body Model (HBM) was developed by the Global Human Body Models
5 Consortium (GHBMC) (Figure 1c). The head region of the model was developed at Wayne
6 State University [36] and the neck region was developed at the University of Waterloo
7 [24,37]. The head and neck model was validated in over 70 cases, including spine-level
8 cases [29] and sled tests considering the whole head and neck model [24,37]. These
9 validation cases include cadaveric testing, and volunteer sled tests which account for
10 muscle activation. The head and neck model of the HBM consists of the entire head and
11 neck and all supporting muscles (Figure 1c), which are constrained to T1 [24].

12 *Helmet Model*

13 The Xenith X2e (V1.0) helmet model was used in the current study (Figure 1d),
14 which includes a chin strap and face mask. Importantly, material samples extracted from
15 this modern football helmet were tested over a large range of rates in both tension and
16 compression to capture the significant viscoelastic effects [38], and experiments were
17 performed on the sub-structures of this helmet at quasi-static and dynamic rates to
18 validate the component models with excellent CORA ratings (0.85 – 0.97) [38]. The full
19 helmet model was validated against 70 experimental configurations with good to
20 excellent correlation ratings, with an average overall CORA rating of 0.82 [27].

1 HBM Positioning

2 The HBM head and neck FE model was assigned the same boundary conditions
3 used in the ATD linear impactor experiment and simulation (Figure 2). The head mass of
4 the HBM was 4.41 kg, which was very similar to that of the ATD (4.54 kg). The moments
5 of inertia of the HBM head ($I_{xx}=18854 \text{ kg mm}^2$, $I_{yy}=22345 \text{ kg mm}^2$, $I_{zz}=17386 \text{ kg mm}^2$) were
6 slightly higher than those of the ATD head ($I_{xx}=15361 \text{ kg mm}^2$, $I_{yy}=21083 \text{ kg mm}^2$, $I_{zz}=18122$
7 kg mm^2) about the local x and y axis (Figure 1c), while the z axis value was slightly lower.
8 Mass was added to the T1 vertebra so that the HBM head and neck FE model had the
9 same combined carriage and neck mass of 19.2 kg used in the ATD experiment and
10 simulation. The T1 was constrained to only translate in the same direction as the impactor
11 translation, as is the case in the linear impactor experimental test setup. A contact friction
12 coefficient of 1.1 was defined between the impactor and the head for the bare-head HBM
13 simulation, and friction coefficients of 0.1 and 0.3 were defined between the impactor
14 and the helmet shell and facemask, respectively. These friction coefficients were
15 consistent with the bare-head and helmeted validation cases used for the helmet model
16 development [27,28].

17 To compare the position and orientation of the HBM and ATD experiment and
18 simulation, the two geometric landmarks used were the neck axis angle (β) and local head
19 x axis angle. The ATD neck axis was well-defined, as it is a cylindrical structure. The
20 coordinate system for the ATD aligned the x axis with the Frankfurt plane [39]. The head
21 of the ATD is angled 4.5 degrees upward relative to the neck. For this study, the neck axis

1 of the HBM was determined by plotting a regression line through the center of gravity
2 (COG) of the seven cervical vertebrae (C1 to C7). In seated position, the neck axis angle
3 was determined to be 0.2° from vertical. The Frankfurt plane of the HBM head was found
4 to be aligned with the local x axis, which is horizontal when the HBM is in the default
5 seated position. To match the ATD, the head of the HBM was repositioned so that the x
6 axis of the head made a 94.5° with the neck axis angle prior to impact. In all HBM
7 simulations, the linear impactor was positioned to match the ATD experiment and
8 simulation, maintaining the same distance offsets relative to the head COG (Figure 2).

9 **Active Musculature**

10 Activation Level (AL) is a dimensionless parameter in the Hill-type muscle
11 elements used in the HBM, representing the level of muscle activation as a function of
12 time. For the current study, only the AL curve for the 1D flexor and extensor muscle
13 elements were modified in the HBM. The AL was assumed to linearly increase from zero
14 at $t = -80$ ms up to a constant maximum value at $t = -60$ ms of $AL = 0.871$, which was the
15 maximum value of the default AL curve, representing the maximum possible level of
16 muscle activation. Two conditions were investigated: (1) a balanced muscle activation
17 scheme (balanced activation), and a (2) baseline condition with no muscle activation (no
18 activation).

19 For the balanced activation condition, the flexor and extensor muscles in the neck
20 were activated at different levels so that the head remained stationary with the same

1 neck axis angle and head x axis angle as that of the ATD and HBM with no activation. The
2 HBM head will rotate relative to the neck and translate forward when the muscles are
3 activated, and the final position of the head depends on the ratio of flexor muscle AL to
4 extensor muscle AL. With the balanced activation scheme, it was confirmed that the head
5 was stationary and in the correct position just prior to impact ($V_{res} < 0.05$ m/s,
6 $\omega_{res} < 0.15$ rad/s). The required ratio of flexor to extensor AL to balance the head and neck
7 in the correct position was 20:3, so the AL curve in the GHMBC model was scaled by a
8 factor of 1.0 for the flexor muscles, and 0.15 for the extensor muscles, which maintained
9 a ratio similar to that suggested by electromyography data for a head up tackle position
10 [40]. For a rugby tackle position with the head up, activation level of the upper, middle
11 and lower trapezius have been shown to be 14%, 37%, and 83% of sternocleidomastoid
12 activation, respectively [40]. The magnitude of flexor AL used ($AL = 0.871$) was
13 approximately 6x the overall level of activation measured in the sternocleidomastoid for
14 a head-up tackle position [40], to represent an high level of muscle activation in the HBM,
15 within physical limits. The impact simulation consisted of an 80 ms delay prior to impact,
16 where the head moved into the desired position (Figure 4) and the helmet was tightened
17 in the helmeted cases, then 30 ms after the time of impact. Prior to impact, the sum of all
18 1D muscle forces at the time of impact was 1.1 kN, at a cross section of the neck 10 mm
19 below the hyoid bone.

20 **Helmet Model Fitting**

1 To fit the helmet to the HBM, a representation of the HBM head geometry, scaled
2 to 0.9x the original size, was first centered inside the helmet model. Over the course of a
3 pre-simulation, the HBM head geometry was expanded to its final geometry, so that the
4 soft foam elements of the helmet model deformed to fit the contours of the head. The
5 same methodology was used previously to fit the helmet to the ATD head, in the
6 development of the helmet model [27]. The final position of the helmet matched the ATD
7 simulation (and experiment) with a distance of 75 mm from the tip of the nose to the
8 brow of the helmet [7]. A penalty-based contact was defined between the HBM head and
9 the helmet with the same friction coefficient of 0.1 used in the ATD simulation [27]. In the
10 helmet model, each chin strap was attached to the helmet shell using a 1D axial element.
11 At the start of the simulation, specific elements were assigned to retract with a specified
12 force, enabling pre-tensioning of the strap system as in the physical tests. This
13 methodology was included in the original helmet model development. Each chin strap
14 was tightened with a force of 50N, which could produce some transient head motion prior
15 to impact. The 80 ms delay prior to impact ensured that the head was stationary based
16 on kinematic criteria ($V_{res} < 0.05$ m/s, $\omega_{res} < 0.15$ rad/s) and in the correct final position at
17 the time of impact.

18 **Model Outputs**

19 The kinematic outputs assessed from the models included the linear acceleration
20 and angular velocity of the head COG. In addition, the lower neck moment and
21 translational acceleration were measured at the T1, and the impactor acceleration and

1 force were reported. The head COG kinematics were measured in the head local
2 coordinate system (Figure 1c), while the other kinematics were resultant values. The
3 acceleration and velocity data from the simulations were processed with a CFC 180 filter,
4 while the force data was processed using a CFC 600 filter, consistent the methods
5 reported in the development of the helmet model. Correlation and Analysis (CORA)
6 software was used to determine how similarly the HBM response compared to the ATD
7 simulation. The kinematic and kinetic responses were assessed by calculating cross-
8 correlation (CORA) values between the response of the ATD simulation to and HBM, using
9 the recommended cross-correlation parameters in the CORA manual [30].

10 Three common head response metrics were investigated, the Head Injury Criteria
11 (HIC), Brain Injury Criteria (BrIC) and Head Impact Power (HIP, calculated using the
12 kinematics of the head COG.

13 The head injury criterion (HIC) (Eqn. 1) is a commonly used metric for head
14 response [41].

$$15 \quad HIC = \max_{t_1, t_2} \left\{ \frac{1}{(t_2 - t_1)^{3/2}} \left[\int_{t_1}^{t_2} a(t) dt \right]^{5/2} \right\} \quad (1)$$

16 Where acceleration is in the units of g , and time is in s . For HIC_{15} , the maximum
17 value of $t_2 - t_1$ is 15 ms.

18 The Brain Injury Criterion (BrIC) (Eqn. 2) is a rotational response criterion
19 determined from the angular velocity of the head. It was developed from a combination
20 of animal response data, ATD testing data, and FE models [34].

$$BrIC = \sqrt{\left(\frac{\omega_x}{\omega_{xC}}\right)^2 + \left(\frac{\omega_y}{\omega_{yC}}\right)^2 + \left(\frac{\omega_z}{\omega_{zC}}\right)^2} \quad (2)$$

Where ω_x , ω_y , and ω_z are the individual peak values of the angular velocity over the entire impact, and ω_{xC} , ω_{yC} , and ω_{zC} are constants equal to 66.2 rad/s, 59.1 rad/s and 44.2 rad/s respectively.

Head Impact Power (HIP) (Eqn. 3) has been correlated with observed concussions in football [42] and considers all 6 degrees-of-freedom.

$$HIP = \max\left[ma_x(t) \int a_x(t)dt + ma_y(t) \int a_y(t)dt + ma_z(t) \int a_z(t)dt + I_{xx}\alpha_x(t) \int \alpha_x(t)dt + I_{yy}\alpha_y(t) \int \alpha_y(t)dt + I_{zz}\alpha_z(t) \int \alpha_z(t)dt\right] \quad (3)$$

Where m is 4.5kg, and I_{xx} , I_{yy} and I_{zz} are 0.016, 0.024 and 0.022 kg m², respectively. These constants represent the mass properties of a 50th percentile male head [42].

The neck compression was also measured for the HBM and the ATD simulation, which was defined as the overall change in length of the neck, measured along the arc of the cervical spine.

RESULTS

The graphical results for head accelerations, angular velocity, reaction moment and impactor force are presented for lateral, frontal and rear helmeted impacts at an impact speed of 5.5 m/s (Figure 5). The complete graphical results are presented in the Supplemental Materials (Figure S5). All head kinematics are stated in the head local

1 coordinate system (Figure 1c). In this section, all cross-correlation (CORA) values were
2 calculated comparing the response of the ATD simulation to the HBM, therefore a cross-
3 correlation value of 1 indicated excellent correspondence between the models, while a
4 cross-correlation value of 0 indicated the ATD simulation and HBM results were not
5 similar.

6 **Comparison of the ATD to the HBM with no activation**

7 Overall, the ATD simulation response was similar to the response of the HBM with
8 no activation. The acceleration in the primary direction of impact (y direction for lateral
9 orientation, x direction for frontal and rear orientation) was similar between the ATD and
10 HBM impacts, with an overall average CORA rating of 0.89 for the bare head cases, and
11 0.90 for the helmeted cases (Table 1). The angular velocity in the primary direction was
12 also similar for the HBM and the ATD (average of 0.88 in the bare head cases, 0.85 for the
13 helmeted cases). In contrast, acceleration in the z direction was not similar between the
14 ATD and HBM, with an overall average rating of 0.43 for the bare-head cases, and 0.42
15 for the helmeted cases. In general, the CORA ratings were higher for the bare head cases
16 than the helmeted cases. The ATD and the HBM ratings indicated a higher degree of
17 correspondence in the lateral orientation compared to the frontal and rear orientations,
18 with all CORA ratings exceeding 0.82 (except z acceleration) in both the bare-head and
19 helmeted cases in the lateral orientation.

1 As expected, the head accelerations and angular velocities increased with
2 increasing impact speed in all impact scenarios. Peak acceleration in the primary impact
3 direction occurred at approximately 4 ms after initial contact for the bare-head cases (see
4 Supplemental Materials, Figure S5) and at approximately 10 ms for the helmeted cases
5 (Figure 5). The HBM had 10% higher peak linear acceleration of the ATD, on average. The
6 HBM reported higher values of HIC compared the ATD (37% , on average), while HIP was
7 only slightly higher (11% on average) and BrIC was slightly lower (4% on average) (Table
8 3). Considering the HBM, HIC was reduced by 46% on average in the helmeted impacts
9 compared to the bare head impacts (Table 3). Early kinematics governed HIC (10-15 ms)
10 and HIP, while the peak values of angular velocity used to calculate BrIC occurred later in
11 the simulation (25 – 30 ms).

12 The neck of HBM deformed considerably more in the axial direction (compression
13 and tension) compared to the ATD neck (Figure 6); the neck of the HBM was stretched or
14 compressed by 8 to 16 mm depending on the orientation, while the neck of the ATD
15 stretched less than 3 mm in all impact orientations.

16 **Comparison of the HBM with and without Muscle Activation**

17 Muscle activation had little influence on the HBM response, indicated by the
18 similar CORA ratings achieved with the “no activation” condition and the “balanced
19 activation” condition. The balanced activation condition caused the average CORA rating
20 to increase (by 1% to 6% for all variables compared to the “no activation” condition,

1 except the primary direction acceleration, which remained the same (Table 1 and Table
2 2). In the bare head cases, CORA ratings for the impactor, and head acceleration and
3 angular velocity in the primary direction decreased by 2% to 4%, while ratings for T1
4 kinematics and z acceleration increased by 3% to 5% with the balanced muscle activation
5 scheme.

6 When comparing the HBM with balanced activation and the HBM with no
7 activation, the former reported 5% lower values of HIC, 3% higher values of BrIC and 2%
8 lower values of HIP on average (Table 3 and Table 4). Interestingly, the HBM with balanced
9 activation reported a higher value of BrIC in the rear and frontal orientations for both the
10 bare head cases (average of 4% and 2% higher respectively), and the helmeted cases
11 (average of 13% and 6% higher, respectively). In the lateral orientation, BrIC was reduced
12 with balanced activation in the bare head (average of 5% lower) and helmeted cases
13 (average of 3% lower), when compared to the HBM with no activation. The largest
14 changes in BrIC due to muscle activation were observed in the lowest severity impacts; in
15 the helmeted impacts at 5.5 m/s, BrIC was reduced by 6% compared to the “no activation”
16 condition, while BrIC increased by 11% in the frontal orientation and 15% in the rear
17 orientation. Considering neck compression, the neck of the HBM with balanced activation
18 was compressed 7 mm by the activation of the muscles, prior to the onset of impact
19 (Figure 6). There was 10 – 20% smaller change in neck compression after the onset of
20 impact in the helmeted impacts with balanced activation compared to the HBM with no
21 activation.

1 **DISCUSSION**

2 The objective of this study was to compare the kinematics of an ATD and a detailed
3 HBM head and neck for linear impactor testing, while varying the impact speed, the
4 impact orientation and the muscle activation in the HBM.

5 **Comparison of the ATD and HBM head and neck kinematics**

6 Overall, the head acceleration in the primary direction from the ATD simulation was
7 similar to that of the HBM with no activation and in all cases, the acceleration peak in the
8 primary direction for the head COG occurred early in time. In all cases, the applied
9 moment about T1, which is found by multiplying impactor force by the perpendicular
10 distance to T1, ranged from 500 – 1500 Nm for the first 8 ms of contact. For the HBM, the
11 measured reaction moment at T1 (Figure 5, Supplemental Materials Figure S5) was always
12 at least 20x lower than the applied moment about T1 during the first 8 ms, and in the ATD
13 simulation the reaction moment at T1 was always at least 6x lower. The considerably
14 lower reaction moment demonstrates that, while the impactor was in contact with the
15 head, the bending stiffness of the neck had little influence on the early kinematics. Since
16 the impact force applied a larger moment than could be resisted by the neck, the mass
17 and local stiffness at the contact site were the main contributors to the early kinematic
18 response. Most of the acceleration peaks occurred during this time, and the angular
19 velocity reached a value near its peak while the impactor was in contact. Comparing the
20 helmeted and bare head cases, the helmeted impacts of the HBM were typically better

1 correlated with the ATD simulation than the bare-head HBM, as indicated by higher CORA
2 ratings. The HBM and ATD helmeted simulations had the same local stiffness properties
3 at the impact site. Conversely, the bare-head HBM and ATD had different soft tissue
4 properties at the location of the impact, resulting in different behavior; the HBM included
5 a biofidelic skin and flesh model while the ATD had a rubber skin covering a metal skull
6 structure.

7 In contrast with the kinematics in the primary direction, large differences in the z
8 axis head acceleration of the HBM and ATD were observed, with the HBM exhibiting
9 higher values. This was caused by the higher axial compliance of the HBM neck, compared
10 to the rubber and metal components in the ATD neck. However, this difference did not
11 contribute to large differences in assessment criteria (HIC, BRIC, HIP) because the peak
12 magnitude of the z acceleration was less than half that of the x acceleration in all HBM
13 impacts. The differences in axial neck compression (Figure 6) should be considered in
14 future studies with impacts directed along the neck. In this study, the neck angle was 15
15 degrees from horizontal, so the majority of the head acceleration was not transmitted
16 axially along the neck. In future studies, especially reconstructions with a striking and
17 struck human surrogate, it will be important to consider the difference in compressive
18 stiffness of the neck between the ATD and HBMs.

19 The HBM head and neck behaved most similarly to the ATD head and neck in the
20 lateral and rear orientation, while it behaved less similarly in the frontal impact. The
21 lateral and rear orientations had impact vectors normal to the struck surface (helmet or

1 head), resulting in minimal sliding during the initial impact in both the ATD and HBM
2 simulation, and subsequently, similar helmet motion. In contrast, the frontal impact
3 exhibited more sliding at the contact surface, in part due to the forward-angled neck and
4 corresponding highly non-normal impact vector. In the bare head impact, the differences
5 in head shape and neck compliance between the ATD and HBM influenced how the
6 impactor first stuck, then slid over the head. In the helmeted frontal impact, the impactor
7 slid over the front edge of the helmet differently in the HBM simulation, compared to the
8 ATD simulation, because the helmet sat slightly differently on the ATD and HBM due to
9 head shape. Post et al. [4] also noted that small changes in helmet geometry at the
10 contact surface had a large influence on helmet motion, and this could be related to the
11 impactor interaction with the helmet. In general, the frontal orientation experienced
12 lower head accelerations. This was thought to be caused by the frontal impact vector
13 acting further from the head COG compared to the lateral and rear impact vectors, which
14 were very close to the head COG.

15 **The effect of muscle activation on head kinematics**

16 The activation of the neck muscles had a very small effect on the kinematics of the
17 head. Although the total active component of the muscle force at the time of impact was
18 approximately 1.1 kN, this force did not result in a large change in the overall head
19 kinematics. Considering the helmeted simulations, the reaction moment at the T1 was
20 only 11% – 16% higher for the HBM with balanced activation compared to the HBM with
21 no activation, despite the large difference in muscle force. Once the contact force from

1 the impactor had dropped later in the impact, the neck musculature then had a larger
2 effect on the resulting kinematics, starting at 20 - 30 ms, which was after most of the peak
3 response metrics had developed.

4 In both the bare head and helmeted cases, the CORA ratings were generally higher
5 for the HBM with balanced activation, compared to the HBM with no activation,
6 suggesting that the ATD was more similar to a human fully braced for impact, attributed
7 to the stiffened neck of the HBM when the muscles are activated. The kinetics and
8 kinematics most affected by active musculature were those measured at T1, which was
9 furthest from the impact site, while those closest to the impact site were affected the
10 least. Active musculature had the largest effect on the motion and moment at the T1
11 (differences of 4 to 6% in the CORA rating), while it had a lesser effect on the primary
12 direction head kinematics (differences ranging from 1 to 4%), and an even smaller effect
13 on the impactor kinematics (0 to 1% difference), on average. The small effect of balanced
14 muscle activation on angular velocity in the current study contrasted somewhat with
15 some of the findings of Jin et al. [14]. The Jin et al. study [14] found that adding muscle
16 activation prior to impact resulted in a 20% reduction on the angular velocity of the head
17 when comparing a HBM with no muscle activation and an HBM with early muscle
18 activation. In the current study, in the helmeted lateral impact at 9.3 m/s, only a 2%
19 decrease was observed in the angular velocity when comparing the HBM with balanced
20 activation to the HBM with no activation. The linear kinematics of this impact were
21 comparable to the impacts by Jin et al. [14] at 9.5 m/s when comparing translational

1 acceleration in the y direction, with a similar peak timing (within 1 ms), value
2 (approximately 1100 m/s²), and subsequent fall to zero (at 20 ms). A possible
3 explanation for the difference in angular velocity reduction between the studies is that
4 the Jin et al. [14] study used the same muscle Activation Level (AL) for the flexor and
5 extensor muscles, which provides much more extensor force than the 0.15:1 ratio used
6 in the current study. If unconstrained, the HBM head would be moving backwards with a
7 significant angular velocity if the flexor and extensor muscles were activated with the
8 same AL curve. The results of the Jin et al. [14] study could be attributed to the head
9 moving into a different position with the early activation scheme that was used. Eckner
10 et al. [23], in which volunteers were tested at non-injurious levels, found a 15% change in
11 head angular velocity due to anticipatory muscle activation, which was a larger effect
12 compared to the current study. The magnitude of the angular velocity in the current study
13 was much higher (8 to 20x) than in the Eckner et al. study, indicating that the applied
14 loading in the current study was much larger. Accordingly, in the current study, muscle
15 activation had a larger influence on BrIC at lower impact speeds. Interestingly, balanced
16 muscle activation slightly increased the peak angular velocity in the frontal and rear
17 orientation in the current study, while peak angular velocity was decreased in the lateral
18 orientation, indicating the need to consider multiple loading directions in future
19 assessment and optimization studies.

20 **Limitations of the study**

1 The implementation of active musculature was a limitation of this study. The Hill-
2 type muscle implementation used in the HBM only changed the axial stiffness of the
3 muscle, not the transverse stiffness. Prescribing the same level of muscle activation to all
4 flexor muscles, and another constant value to all extensor muscles, was a simplification.
5 More electromyography data on football-specific muscle activation, and more detailed
6 implementation in the FE model will improve the predictive outcome of these models.
7 Notwithstanding, it was apparent that the contribution of active musculature was small
8 in the linear impactor test.

9 The construction of the linear impactor created a challenging boundary condition
10 in the frontal impact orientation, where there was considerable sliding, shearing and
11 sometimes detachment of the impactor end cap and foam. The physical impactor
12 comprised of three components attached together with Velcro. In the lateral and rear
13 impacts, this resulted in relatively little shearing of the foam and a predominantly
14 compressive load to the impactor. In the frontal impact, the impactor experienced tension
15 and compression, which resulted in the Velcro disconnecting and in some cases the
16 impactor foam separated completely from the impactor later in the impact (always >25ms
17 after impact), which was not modelled in the simulation. The Velcro was modelled using
18 a tied contact in the simulations, which may have induced some tensile force in the
19 impactor. Even so, the average CORA rating of 0.82 [28] comparing the bare-head
20 experiment and simulation of the ATD linear impactor test indicated that the response of
21 the head was in good agreement with the experiment.

1 **CONCLUSIONS**

2 The ATD head and neck provided a similar estimate of head kinematics in a linear
3 impactor test, when compared to a more detailed HBM, for both bare-head and helmeted
4 impact. The prediction of head response metrics was similar for both models. In both the
5 HBM and the ATD, the helmet reduced two kinematic response predictors by 38 to 50 %
6 over the range of speeds and orientations, when compared to a bare-head impact with
7 the same compliant impactor.

8 1. The contribution of muscle activation to head kinematics was found to be
9 relatively small in the current study, using a balanced muscle activation scheme.

10 This was because the peak accelerations developed early in time, when the
11 impactor force greatly exceeded the resisting moment from the neck, and the
12 kinematics of the head were dominated by the mass and local stiffness properties
13 of the head, impactor and where applicable, the helmet.

14 2. The HBM with no muscle activation was found to have similar linear head
15 acceleration to the ATD simulation in the primary impact direction, with the
16 acceleration-time history receiving average CORrelation and Analysis (CORA)
17 ratings of 0.89 and 0.90 comparing the bare-head and helmeted impacts,
18 respectively, indicating good overall correlation. The primary direction angular
19 velocity of the head was also similar, with average CORA ratings of 0.88 (bare-
20 head) and 0.85 (helmeted) considering all impact orientations.

- 1 3. Comparing all helmeted and bare-head impacts of the HBM with no muscle
2 activation to the ATD simulation, the z acceleration of the head was considerably
3 lower in the ATD compared to the HBM, with average CORA ratings of 0.43 (bare-
4 head) and 0.42 (helmeted). In addition, the axial stretching and compression of
5 the ATD neck was much less than that of the HBM. Although the overall magnitude
6 of the z acceleration was less than the x acceleration in the current study, the
7 results imply that using an ATD to represent an impact with a large z component
8 could result in a less biofidelic kinematic response.
- 9 4. When assessing head response based on peak acceleration, it was found that the
10 bending stiffness of the neck did not play a strong role, within the range of impacts
11 that were examined with the ATD and the HBM in the current study.

12 **ACKNOWLEDGMENT**

13 The authors would like to acknowledge the Global Human Body Models
14 Consortium for use of the 50th percentile male head-and-neck model, and Biocore LLC for
15 the use of the ATD linear impactor test model, Xenith X2e helmet model and experimental
16 validation data. The authors would like to thank Compute Canada and SHARCNet for
17 providing the necessary computing resources.

18 **FUNDING**

1 The research presented in this paper was made possible by a grant from Football
2 Research, Inc. (FRI). The views expressed are solely those of the authors and do not
3 represent those of FRI or any of its affiliates or funding sources.

4 REFERENCES

- 5 [1] Hoshizaki, T. B., Brien, S. E., Bailes, J. E., Maroon, J. C., Kaye, A. H., and Cantu, R.
6 C., 2004, "The Science and Design of Head Protection in Sport," *Neurosurgery*,
7 **55**(4), pp. 956–967.
- 8 [2] Gwin, J. T., Chu, J. J., Diamond, S. G., Halstead, P. D., Crisco, J. J., and Greenwald,
9 R. M., 2010, "An Investigation of the NOCSAE Linear Impactor Test Method Based
10 on In Vivo Measures of Head Impact Acceleration in American Football," *J.*
11 *Biomech. Eng.*, **132**(1), p. 011006.
- 12 [3] Viano, D. C., Withnall, C., and Halstead, D., 2012, "Impact Performance of Modern
13 Football Helmets," *Ann. Biomed. Eng.*, **40**(1), pp. 160–174.
- 14 [4] Post, A., Oeur, A., Hoshizaki, B., and Gilchrist, M. D., 2013, "An Examination of
15 American Football Helmets Using Brain Deformation Metrics Associated with
16 Concussion," *Mater. Des.*, **45**, pp. 653–662.
- 17 [5] NOCSAE, 2017, "Standard Performance Specification for Newly Manufactured
18 Football Helmets," pp. 2–6 [Online]. Available:
19 [https://nocsae.org/standard/standard-performance-specification-for-newly-](https://nocsae.org/standard/standard-performance-specification-for-newly-manufactured-football-helmets-3/)
20 [manufactured-football-helmets-3/](https://nocsae.org/standard/standard-performance-specification-for-newly-manufactured-football-helmets-3/).
- 21 [6] Elkin, B. S., Gabler, L. F., Panzer, M. B., and Siegmund, G. P., 2018, "Brain Tissue
22 Strains Vary with Head Impact Location: A Possible Explanation for Increased
23 Concussion Risk in Struck versus Striking Football Players," *Clin. Biomech.*,
24 (January), pp. 1–9.
- 25 [7] Funk, J. R., Crandall, J., Wonnacott, M., and Withnall, C., 2017, *Linear Impactor*
26 *Helmet Test Protocol*.
- 27 [8] Pellman, E. J., Viano, D. C., Withnall, C., Shewchenko, N., Bir, C. A., and Halstead,
28 P. D., 2006, "Concussion in Professional Football: Helmet Testing to Assess Impact
29 Performance - Part 11," *Neurosurgery*, **58**(1), pp. 78–95.
- 30 [9] Marjoux, D., Baumgartner, D., Deck, C., and Willinger, R., 2008, "Head Injury
31 Prediction Capability of the HIC, HIP, SIMon and ULP Criteria," *Accid. Anal. Prev.*,
32 **40**(3), pp. 1135–1148.
- 33 [10] Withnall, C., Shewchenko, N., Gittens, R., and Dvorak, J., 2005, "Biomechanical

- 1 Investigation of Head Impacts in Football,” *Br. J. Sports Med.*, **39**(SUPPL. 1), pp.
2 49–58.
- 3 [11] Gabler, L. F., Crandall, J. R., and Panzer, M. B., 2016, “Assessment of Kinematic
4 Brain Injury Metrics for Predicting Strain Responses in Diverse Automotive Impact
5 Conditions,” *Ann. Biomed. Eng.*, **44**(12), pp. 3705–3718.
- 6 [12] Post, A., Oeur, A., Walsh, E., Hoshizaki, B., and Gilchrist, M. D., 2014, “A
7 Centric/Non-Centric Impact Protocol and Finite Element Model Methodology for
8 the Evaluation of American Football Helmets to Evaluate Risk of Concussion,”
9 *Comput. Methods Biomech. Biomed. Engin.*, **17**(16), pp. 1785–1800.
- 10 [13] Kallieris, D., Rizzetti, A., and Mattern, R., 1995, “The Biofidelity of Hybrid III
11 Dummies,” *International Research Council on Biomechanics of Injury*, IRCOBI, pp.
12 135–154.
- 13 [14] Jin, X., Feng, Z., Mika, V. H., Li, H., Viano, D., and Yang, K. H., 2017, “The Role of
14 Neck Muscle Activities on the Risk of Mild Traumatic Brain Injury in American
15 Football,” *J. Biomech. Eng.*, **139**(October 2017).
- 16 [15] Karton, C. M., Hoshizaki, T. B., and Gilchrist, M. D., 2014, “The Influence of
17 Impactor Mass on the Dynamic Response of the Hybrid III Headform and Brain
18 Tissue Deformation,” *Mech. Concussion Sport.*, **40**(STP1552), pp. 23–40.
- 19 [16] Viano, D. C., Casson, I. R., Pellman, E. J., Zhang, L., King, A. I., and Yang, K. H.,
20 2005, “Concussion in Professional Football: Brain Responses by Finite Element
21 Analysis: Part 9,” *Neurosurgery*, **57**(5), pp. 891–915.
- 22 [17] Johnson, K. L., Chowdhury, S., Lawrimore, W. B., Mao, Y., Mehmani, A., Prabhu,
23 R., Rush, G. A., and Horstemeyer, M. F., 2016, “Constrained Topological
24 Optimization of a Football Helmet Facemask Based on Brain Response,” *Mater.
25 Des.*, **111**, pp. 108–118.
- 26 [18] Darling, T., Muthuswamy, J., and Rajan, S. D., 2016, “Finite Element Modeling of
27 Human Brain Response to Football Helmet Impacts,” *Comput. Methods Biomech.
28 Biomed. Engin.*, **19**(13), pp. 1432–1442.
- 29 [19] (GHBMC), G. H. B. M. C., 2019, “Resources” [Online]. Available:
30 <https://www.elemance.com/resources/>.
- 31 [20] Rush, G. A., 2016, “Design of an American Football Helmet Liner for Concussion
32 Mitigation,” Mississippi State University, Mississippi, USA.
- 33 [21] Craig, M. J., 2007, “Biomechanics of Jaw Loading in Football Helmet Impacts,”
34 Wayne State University, Detroit, Michigan, USA.
- 35 [22] Schmidt, J. D., Guskiewicz, K. M., Blackburn, J. T., Mihalik, J. P., Siegmund, G. P.,
36 and Marshall, S. W., 2014, “The Influence of Cervical Muscle Characteristics on

- 1 Head Impact Biomechanics in Football,” *Am. J. Sports Med.*, **42**(9), pp. 2056–
2 2066.
- 3 [23] Eckner, J. T., Oh, Y. K., Joshi, M. S., Richardson, J. K., and Ashton-Miller, J. A., 2014,
4 “Effect of Neck Muscle Strength and Anticipatory Cervical Muscle Activation on
5 the Kinematic Response of the Head to Impulsive Loads,” *Am. J. Sports Med.*,
6 **42**(3), pp. 566–576.
- 7 [24] Fice, J. B., Cronin, D. S., and Panzer, M. B., 2011, “Cervical Spine Model to Predict
8 Capsular Ligament Response in Rear Impact,” *Ann. Biomed. Eng.*, **39**(8), pp. 2152–
9 2162.
- 10 [25] Cronin, D. S., and Barker, J. B., 2018, “Investigation of Kinematic and Tissue-Level
11 Response Using a 50th Percentile Male Neck Finite Element Model,” *Human*
12 *Modeling Symposium*, Berlin.
- 13 [26] Bruneau, D., Cronin, D., Giudice, J. S., Panzer, M. B., and Kent, R., 2018,
14 “Comparison of the Hybrid III Head and Neck to a Detailed Head and Neck Finite
15 Element Model with Active Musculature, in a Football Impact Scenario,” *IRCOBI*,
16 pp. 322–323.
- 17 [27] Cronin, D., Barker, J., Gierczycka, D., Bruneau, D., Bustamante, M., and Corrales,
18 M., 2018, “User Manual - Finite Element Model of 2016 Xenith X2E (Safety
19 Equipment Institute Model X2E) Version 1.0 for LS-DYNA” [Online]. Available:
20 <http://biocorellc.com/resources/>.
- 21 [28] Giudice, J. S., Park, G., Kong, K., Bailey, A., Kent, R., and Panzer, M. B., 2018,
22 “Development of Open-Source Dummy and Impactor Models for the Assessment
23 of American Football Helmet Finite Element Models,” *Ann. Biomed. Eng.*, (434),
24 pp. 1–27.
- 25 [29] Barker, J. B., Cronin, D. S., and Nightingale, R. W., 2017, “Lower Cervical Spine
26 Motion Segment Computational Model Validation: Kinematic and Kinetic
27 Response for Quasi-Static and Dynamic Loading,” *J. Biomech. Eng.*, **139**(6), p.
28 061009.
- 29 [30] Thunert, C., 2012, “CORA Release 3.6 User’s Manual” [Online]. Available:
30 <http://www.pdb-org.com/en/information/18-cora-download.html>.
- 31 [31] White, N. A., Danelson, K. A., Scott Gayzik, F., and Stitzel, J. D., 2014, “Head and
32 Neck Response of a Finite Element Anthropomorphic Test Device and Human
33 Body Model During a Simulated Rotary-Wing Aircraft Impact,” *J. Biomech. Eng.*,
34 **136**(11), p. 111001.
- 35 [32] Vavalle, N. A., Jelen, B. C., Moreno, D. P., Stitzel, J. D., and Gayzik, F. S., 2013, “An
36 Evaluation of Objective Rating Methods for Full-Body Finite Element Model
37 Comparison to PMHS Tests,” *Traffic Inj. Prev.*, **14**(SUPPL1).

- 1 [33] Gennarelli, T. A., Thibault, L. E., Adams, J. H., Graham, D. I., Thompson, C. J., and
2 Marcincin, R. P., 1982, "Diffuse Axonal Injury and Traumatic Coma in the
3 Primate," *Ann. Neurol.*, **12**(6), pp. 564–574.
- 4 [34] Takhounts, E. G., Craig, M. J., Moorhouse, K., McFadden, J., and Hasija, V., 2013,
5 "Development of Brain Injury Criteria (BrIC)," *Stapp Car Crash J.*, **57**(November),
6 p. 243.
- 7 [35] Broglio, S. P., Sosnoff, J. J., Shin, S., He, X., Alcaraz, C., and Zimmerman, J., 2009,
8 "Head Impacts During High School Football: A Biomechanical Assessment," **44**(4),
9 pp. 342–349.
- 10 [36] Mao, H., Zhang, L., Jiang, B., Genthikatti, V. V., Jin, X., Zhu, F., Makwana, R., Gill,
11 A., Jandir, G., Singh, A., and Yang, K. H., 2013, "Development of a Finite Element
12 Human Head Model Partially Validated With Thirty Five Experimental Cases," *J.*
13 *Biomech. Eng.*, **135**(11), p. 111002.
- 14 [37] Panzer, M. B., Fice, J. B., and Cronin, D. S., 2011, "Cervical Spine Response in
15 Frontal Crash," *Med. Eng. Phys.*, **33**(9), pp. 1147–1159.
- 16 [38] Bustamante, M. C. , Bruneau, D. , Barker, J. B. , Gierczycka, D. , Corrales, M. A. , &
17 Cronin, D. S., "Component-Level Finite Element Model and Validation for a
18 Modern American Football Helmet. *Journal of Dynamic Behavior of Materials*
19 (Accepted)," *J. Dyn. Behav. Mater.*
- 20 [39] Yoganandan, N., Pintar, F. A., Zhang, J., and Baisden, J. L., 2009, "Physical
21 Properties of the Human Head: Mass, Center of Gravity and Moment of Inertia,"
22 *J. Biomech.*, **42**(9), pp. 1177–1192.
- 23 [40] Morimoto, K., Sakamoto, M., Fukuhara, T., and Kato, K., 2013,
24 "Electromyographic Study of Neck Muscle Activity According to Head Position in
25 Rugby Tackles," *J. Phys. Ther. Sci.*, **25**(5), pp. 563–566.
- 26 [41] Hutchinson, J., Kaiser, M. J., and Lankarani, H. M., 1998, "The Head Injury
27 Criterion (HIC) Functional," *Appl. Math. Comput.*, **96**(1), pp. 1–16.
- 28 [42] Hernandez, F., Wu, L. C., Yip, M. C., Laksari, K., Hoffman, A. R., Lopez, J. R., Grant,
29 G. A., Kleiven, S., and Camarillo, D. B., 2015, "Six Degree-of-Freedom
30 Measurements of Human Mild Traumatic Brain Injury," *Ann. Biomed. Eng.*, **43**(8),
31 pp. 1918–1934.

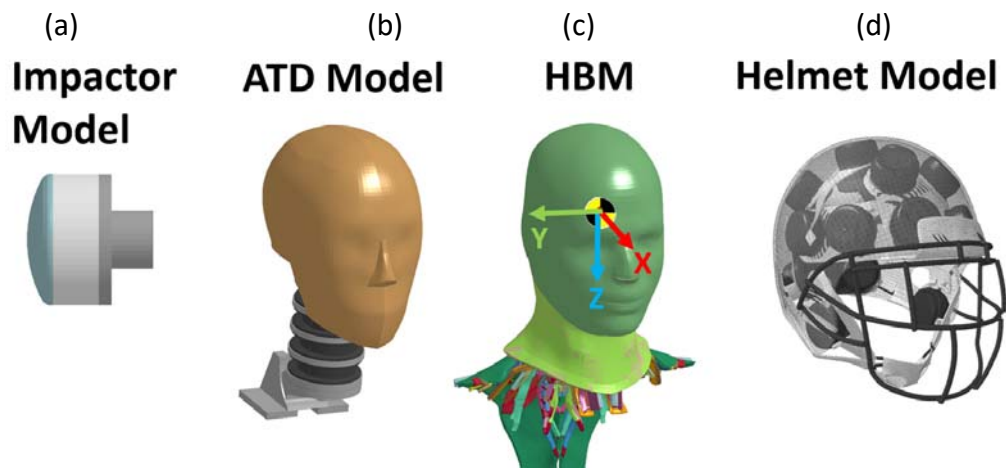
32

33

1 Figure Captions List

- Fig. 1 Existing Models: (a) Deformable Impactor Model, (b) ATD Model, (c) Human Body Model (showing local coordinate system), (d) Helmet Model
- Fig. 2 (a) Boundary conditions of the simulated linear impactor tests, (b) table of dimensional offsets for each orientation, given in the global coordinate system
- Fig. 3 Test matrix, showing all 54 simulated impacts
- Fig. 4 Main simulation timeline, for “balanced activation” condition in a frontal impact at 5.5 m/s (a) bare head, (b) helmeted
- Fig. 5 Helmeted Impact Kinematics, 5.5 m/s, (a) Lateral, (b) Frontal, (c) Rear
- Fig. 6 Neck Compression in helmeted impact (a) lateral, (b) frontal, and (c) rear helmeted impact at 5.5 m/s

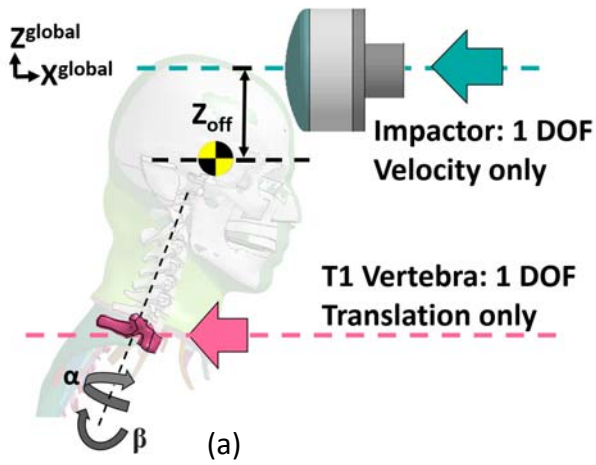
2



1

2 **Figure 1 Existing Models: (a) Deformable Linear Impactor Model, (b) ATD Model, (c) Human Body Model**
3 **(showing local coordinate system), (d) Helmet Model**

4



	Lateral	Frontal	Rear
Y_{off}	-6 mm	1 mm	1 mm
Z_{off}	6 mm	70 mm	9 mm
α (°)	-95°	0°	180°
β (°)	11°	15°	-15°

1

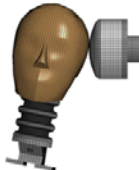


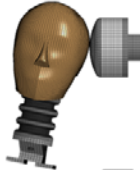
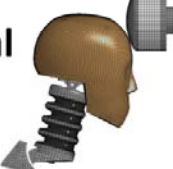


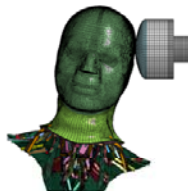

(b)

2 Figure 2 (a) Boundary conditions of the simulated linear impactor tests, (b) table of dimensional offsets
 3 for each orientation, given in the global coordinate system

4

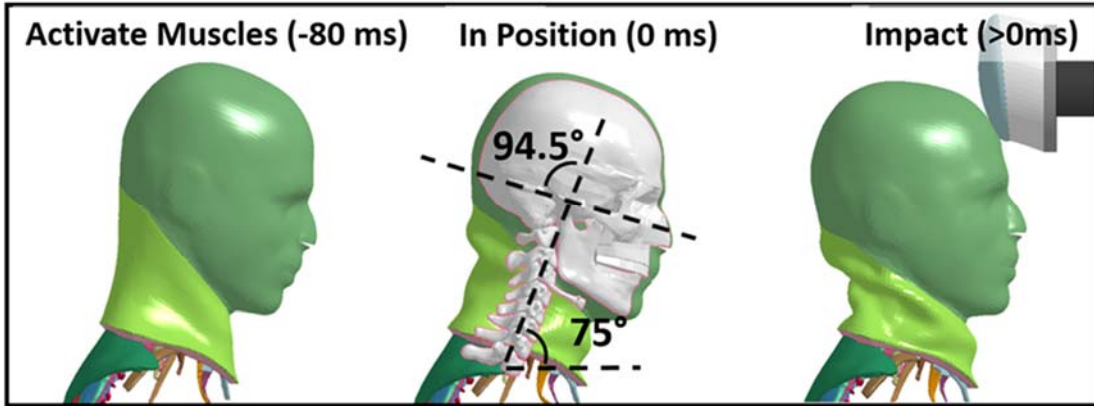
5

6

3x Finite Element Models	3x Orientations	3x Impact Velocities	2x Configurations
<p>ATD Simulation </p> <p>HBM - No Activation </p> <p>HBM - Balanced Activation </p>	<p>Lateral </p> <p>Frontal </p> <p>Rear </p>	<p> v</p> <p>5.5 m/s 7.4 m/s 9.3 m/s</p>	<p>Bare Head </p> <p>Helmeted </p>

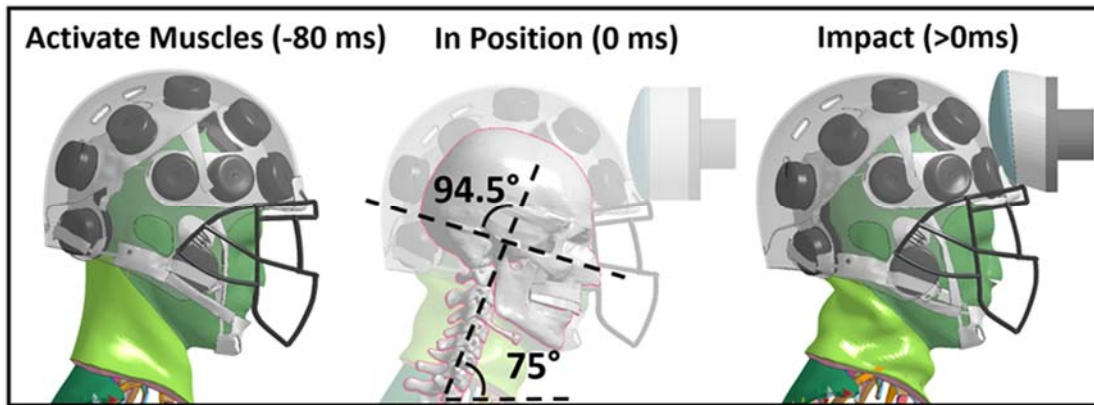
1
2
3
4

Figure 3 Test matrix, showing all 54 simulated impacts



1

(a)



2

3

4

(b)Figure 4 Main simulation timeline, for “balanced activation” condition in a frontal impact at 5.5 m/s (a) bare head, (b) helmeted

5

6

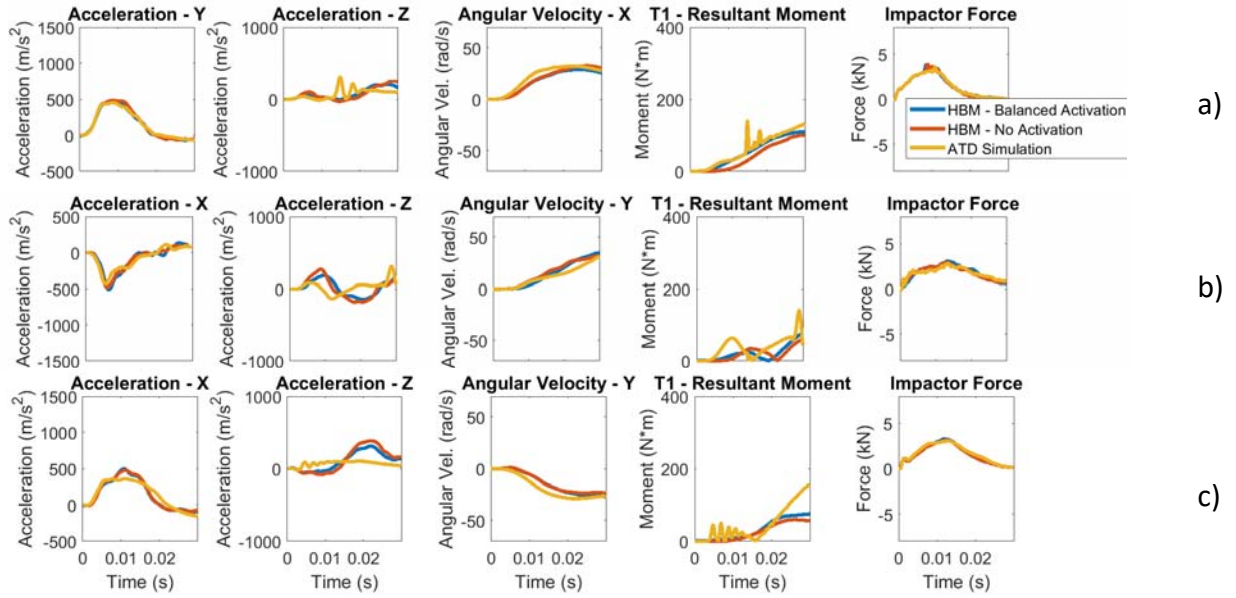
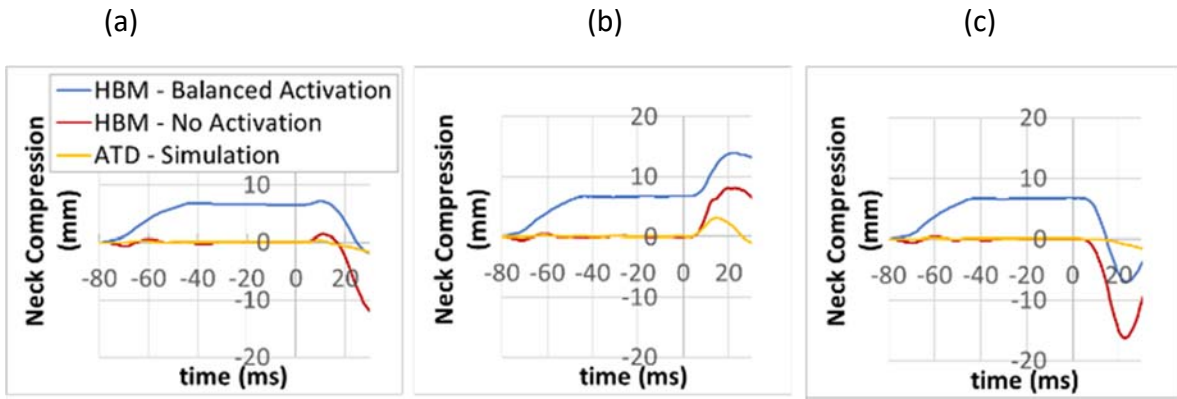


Figure 5 Helmeted Impact Kinematics, 5.5 m/s, (a) Lateral, (b) Frontal, (c) Rear

1

2



1

2 Figure 6 Neck Compression in helmeted impact (a) lateral, (b) frontal, and (c) rear helmeted impact at
 3 5.5 m/s

4

5

6

7

8

9

10

11

12

13

14

15

16

17

18

19

20

21

22

23

24

25

26

1 Table Caption List

Table 1	CORA ratings between HBM simulations and ATD simulations with no activation
Table 2	CORA ratings between HBM simulations and ATD simulations with balanced activation
Table 3	Response Metrics of HBM: HIC, BrIC and HIP, and ratio of HBM with no activation to ATD simulation response (bold indicates average response)
Table 4	Response Metrics of HBM: HIC, BrIC and HIP, and ratio of HBM with balanced activation to ATD simulation response (bold indicates average response)

2
3
4
5
6
7

1

Configuration	Orientation	Speed	Head COG					T1		Impactor		
			Acc. X	Acc. Y	Acc. Z	Ang. Vel. X	Ang. Vel. Y	Acc.	M _{res}	Acc.	F _{res}	
Bare Head	Lateral	5.5 m/s	-	0.93	0.46	0.97	-	0.79	0.84	0.87	0.97	
		7.4 m/s	-	0.93	0.52	0.95	-	0.84	0.83	0.88	0.96	
		9.3 m/s	-	0.93	0.56	0.94	-	0.87	0.79	0.92	0.96	
		Average	-	0.93	0.51	0.95	-	0.83	0.82	0.89	0.96	
	Frontal	5.5 m/s	0.92	-	0.33	-	0.81	0.69	0.28	0.83	0.81	
		7.4 m/s	0.84	-	0.38	-	0.82	0.64	0.57	0.73	0.81	
		9.3 m/s	0.69	-	0.47	-	0.83	0.47	0.54	0.58	0.65	
		Average	0.82	-	0.39	-	0.82	0.6	0.46	0.71	0.76	
	Rear	5.5 m/s	0.93	-	0.33	-	0.88	0.58	0.50	0.85	0.96	
		7.4 m/s	0.93	-	0.39	-	0.87	0.64	0.47	0.86	0.96	
		9.3 m/s	0.95	-	0.46	-	0.85	0.72	0.45	0.90	0.95	
		Average	0.94	-	0.39	-	0.87	0.65	0.47	0.87	0.96	
	Average			0.89		0.43		0.88	0.69	0.59	0.82	0.89
	Helmet	Lateral	5.5 m/s	-	0.96	0.49	0.93	-	0.94	0.82	0.95	0.98
			7.4 m/s	-	0.96	0.52	0.93	-	0.98	0.82	0.95	0.99
9.3 m/s			-	0.95	0.50	0.94	-	0.96	0.82	0.97	0.98	
Average			-	0.96	0.50	0.93	-	0.96	0.82	0.95	0.98	
Frontal		5.5 m/s	0.89	-	0.36	-	0.82	0.74	0.47	0.84	0.96	
		7.4 m/s	0.8	-	0.38	-	0.72	0.70	0.53	0.65	0.63	
		9.3 m/s	0.78	-	0.44	-	0.75	0.61	0.58	0.67	0.67	
		Average	0.82	-	0.40	-	0.76	0.68	0.53	0.72	0.75	
Rear		5.5 m/s	0.88	-	0.36	-	0.88	0.88	0.51	0.96	0.97	
		7.4 m/s	0.93	-	0.34	-	0.84	0.88	0.47	0.94	0.97	
		9.3 m/s	0.96	-	0.35	-	0.84	0.80	0.48	0.91	0.96	
		Average	0.93	-	0.35	-	0.85	0.85	0.49	0.93	0.97	
Average			0.90		0.42		0.85	0.83	0.61	0.87	0.90	

2 Table 1 CORA ratings between HBM simulations and ATD simulations with no activation

3

1

Configuration	Orientation	Speed	Head COG					T1		Impactor	
			Acc. X	Acc. Y	Acc. Z	Ang. Vel. X	Ang. Vel. Y	Acc.	M _{res}	Acc.	F _{res}
Bare Head	Lateral	5.5 m/s	-	0.91	0.60	0.94	-	0.83	0.97	0.84	0.93
		7.4 m/s	-	0.92	0.58	0.93	-	0.87	0.89	0.86	0.93
		9.3 m/s	-	0.84	0.59	0.91	-	0.92	0.81	0.80	0.85
		Average	-	0.89	0.59	0.93	-	0.87	0.89	0.83	0.90
	Frontal	5.5 m/s	0.95	-	0.35	-	0.76	0.79	0.35	0.86	0.84
		7.4 m/s	0.85	-	0.39	-	0.80	0.76	0.64	0.76	0.83
		9.3 m/s	0.67	-	0.50	-	0.83	0.56	0.59	0.55	0.65
		Average	0.82	-	0.41	-	0.80	0.70	0.53	0.72	0.77
	Rear	5.5 m/s	0.92	-	0.34	-	0.87	0.64	0.54	0.83	0.90
		7.4 m/s	0.90	-	0.39	-	0.86	0.67	0.49	0.83	0.87
		9.3 m/s	0.87	-	0.43	-	0.84	0.69	0.45	0.79	0.84
		Average	0.90	-	0.39	-	0.86	0.67	0.49	0.82	0.87
Average			0.87	0.46	0.86	0.75	0.64	0.79	0.85		
Helmet	Lateral	5.5 m/s	-	0.99	0.57	0.91	-	0.87	0.92	0.96	0.98
		7.4 m/s	-	0.99	0.61	0.91	-	0.98	0.87	0.96	0.98
		9.3 m/s	-	0.97	0.59	0.93	-	0.97	0.78	0.89	0.99
		Average	-	0.98	0.59	0.92	-	0.94	0.86	0.94	0.98
	Frontal	5.5 m/s	0.84	-	0.43	-	0.89	0.77	0.61	0.91	0.94
		7.4 m/s	0.77	-	0.41	-	0.85	0.75	0.69	0.81	0.64
		9.3 m/s	0.78	-	0.48	-	0.85	0.70	0.68	0.70	0.79
		Average	0.79	-	0.44	-	0.86	0.74	0.66	0.81	0.79
	Rear	5.5 m/s	0.88	-	0.42	-	0.88	0.94	0.53	0.93	0.97
		7.4 m/s	0.93	-	0.37	-	0.85	0.88	0.48	0.95	0.98
		9.3 m/s	0.96	-	0.37	-	0.85	0.83	0.47	0.93	0.97
		Average	0.93	-	0.39	-	0.86	0.88	0.49	0.93	0.97
Average			0.90	0.47	0.88	0.85	0.67	0.89	0.91		

2 Table 2 CORA ratings between HBM simulations and ATD simulations with balanced activation

3

1

Configuration	Orientation	Speed	HIC ₁₅ (HBM)	HBM/ATD (HIC ₁₅)	BrIC (HBM)	HBM/ATD (BrIC)	HIP (W) (HBM)	HBM/ATD (HIP)
Bare Head	Lateral	5.5 m/s	348	1.29	0.53	0.90	15651	1.16
		7.4 m/s	658	1.23	0.68	0.96	24871	1.10
		9.3 m/s	1095	1.18	0.82	0.95	38225	1.07
			Average	1.23		0.93		1.11
	Frontal	5.5 m/s	183	1.15	0.45	0.92	9716	0.79
		7.4 m/s	367	1.06	0.62	0.89	16217	0.76
		9.3 m/s	647	0.92	0.88	0.82	26442	0.56
			Average	1.04		0.88		0.93
	Rear	5.5 m/s	364	1.11	0.52	0.95	14977	0.64
		7.4 m/s	671	1.11	0.71	0.95	24489	0.67
		9.3 m/s	1133	1.05	0.75	0.79	39356	0.69
			Average	1.09		0.90		1.02
Average				1.12		0.90		1.02
Helmet	Lateral	5.5 m/s	133	1.14	0.51	1.00	8357	1.19
		7.4 m/s	264	1.09	0.64	1.01	14928	1.12
		9.3 m/s	586	1.18	0.74	1.01	26462	1.07
			Average	1.13		1.01		1.13
	Frontal	5.5 m/s	117	1.74	0.53	1.01	5250	1.27
		7.4 m/s	244	1.56	0.73	0.95	11574	1.02
		9.3 m/s	427	1.40	0.91	0.94	19465	1.05
			Average	1.57		0.96		1.11
	Rear	5.5 m/s	152	1.63	0.40	0.82	8055	1.23
		7.4 m/s	394	1.52	0.59	0.98	17588	1.04
		9.3 m/s	650	1.08	0.65	0.90	26869	0.96
			Average	1.41		0.90		1.08
Average				1.37		0.96		1.11

2 Table 3 Response Metrics of HBM: HIC, BrIC and HIP, and ratio of HBM with no activation to ATD
 3 simulation response (bold indicates average response)

4

1

Configuration	Orientation	Speed	HIC ₁₅ (HBM)	HBM/ATD (HIC ₁₅)	BrIC (HBM)	HBM/ATD (BrIC)	HIP (W) (HBM)	HBM/ATD (HIP)	
Bare Head	Lateral	5.5 m/s	342	1.26	0.50	0.85	15350	1.13	
		7.4 m/s	644	1.21	0.65	0.91	24353	1.08	
		9.3 m/s	1085	1.17	0.78	0.91	37936	1.06	
			Average		1.21		0.89		1.09
	Frontal	5.5 m/s	180	1.13	0.49	1.00	9719	0.79	
		7.4 m/s	362	1.04	0.62	0.89	16208	0.76	
		9.3 m/s	627	0.89	0.86	0.81	25777	0.56	
			Average		1.02		0.90		0.93
	Rear	5.5 m/s	352	1.07	0.52	0.96	14692	0.64	
		7.4 m/s	649	1.07	0.69	0.92	23840	0.67	
		9.3 m/s	1098	1.02	0.85	0.89	38164	0.69	
			Average		1.05		0.92		0.99
Average				1.10		0.90		1.00	
Helmet	Lateral	5.5 m/s	112	0.96	0.48	0.95	6944	0.99	
		7.4 m/s	225	0.93	0.62	0.98	12957	0.97	
		9.3 m/s	550	1.11	0.73	0.99	25493	1.03	
			Average		1.00		0.97		1.00
	Frontal	5.5 m/s	106	1.57	0.59	1.11	5677	0.79	
		7.4 m/s	237	1.51	0.76	0.99	11963	0.76	
		9.3 m/s	434	1.42	0.93	0.96	20776	0.56	
			Average		1.50		1.02		1.18
	Rear	5.5 m/s	124	1.33	0.46	0.94	7748	0.64	
		7.4 m/s	347	1.34	0.63	1.04	17126	0.67	
		9.3 m/s	672	1.12	0.76	1.06	25685	0.69	
			Average		1.26		1.01		1.04
Average				1.25		1.00		1.07	

2 Table 4 Response Metrics of HBM: HIC, BrIC and HIP, and ratio of HBM with balanced activation
 3 compared to ATD simulation response (bold indicates average response)

4

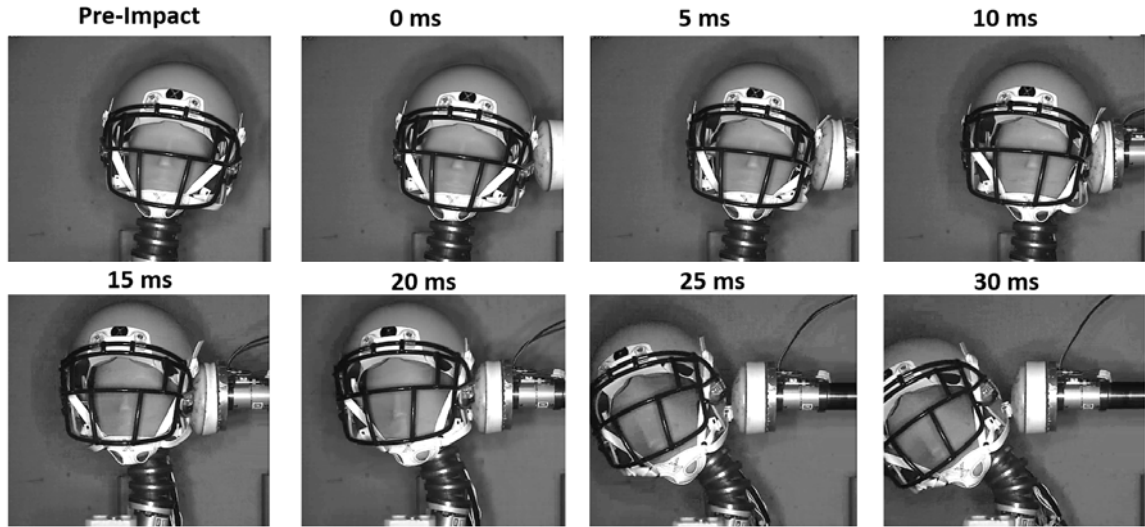
5

6

7

1 **SUPPLEMENTAL MATERIALS**

2 **Linear Impactor Test**



3

4 **Figure S1** Typical time history of an experimental linear impactor test, shown in the lateral orientation
 5 at 9.3 m/s

6 **Finite Element Modelling Details**

7 The impactor model consists of 9409 elements total.

Component	Material	Element Type	Material Model	Visco-elastic?
Foam Disc	Vinyl-Nitrile Foam	Solid	Fu-Chang Foam (*MAT_181)	Yes
End Cap	Nylon	Solid	Elastic (*MAT_001)	No
Ram	Metal	Solid	Rigid	No

8 **Table S1** Impactor Model Details

9 The Hybrid III anthropometric testing device model consists of 57762 elements total.

Component	Material	Element Type	Material Model	Visco-elastic?
Skull	Aluminum	Solid	Elastic (*MAT_001)	No

Skin	Soft Vinyl	Solid	Hyperelastic rubber (*MAT_181)	No
Neck Discs/Mount	Steel/Aluminum	Solid	Rigid	No
Neck Cable	Steel	Axial	Elastic (*MAT_001)	No
Neck Rubber	Butyl Rubber	Solid	Viscous Foam (*MAT_062)	Yes

1 **Table S2 Hybrid III ATD Model Details**

2 The human body model consists of 482257 elements total.

Region	Part	Element Type	Material Model	Visco-elastic?
Outer Tissue	Skin	Shell	Linear viscoelastic (*MAT_006)	Yes
	Subcutaneous Tissue	Solid	Hyperelastic rubber (*MAT_181)	No
Soft Tissue - Head	Brain Tissue	Solid	Linear Viscoelastic (*MAT_061)	Yes
	Lateral Ventricle, CSF	Solid	Linear Viscoelastic (*MAT_061)	Yes
	Meninges	Shell	Elastic (*MAT_001)	No
	Bridging Veins	Beam	Elasto-Plastic (*MAT_024)	No
Soft Tissue - Neck	Passive Muscle	Solid	Viscoelastic Ogden (*MAT_77_O)	Yes
	Active Muscle Attachments	Beam	Discrete Spring (*MAT_074)	No
	Anterior Tissue	Shell	Hyperelastic rubber (*MAT_181)	No
	Hyoid Inferior/Superior Springs	Axial	Elastic spring (*MAT_S01)	No
Skull	Skull	Solid	Elasto-Plastic (*MAT_024) and Elastic (*MAT_001)	No
	Teeth	Solid	Rigid	-
Cervical Spine	Ligaments	Axial	Discrete Spring (*MAT_074)	Yes
	Annulus Matrix	Solid	Hill Compressible Foam (*MAT_177)	No
	Nucleus 3D	Solid	Elastic Fluid (MAT_001_Fluid)	Yes
	Fibrosis	Shell	Fabric (*MAT_034)	No
	Cortical Bone	Shell	Bi-Linear Plastic (*MAT_003)	No
	Trabecular Bone	Solid	Bi-Linear Plastic (*MAT_003)	No

3 **Table S3 Human Body Model Details**

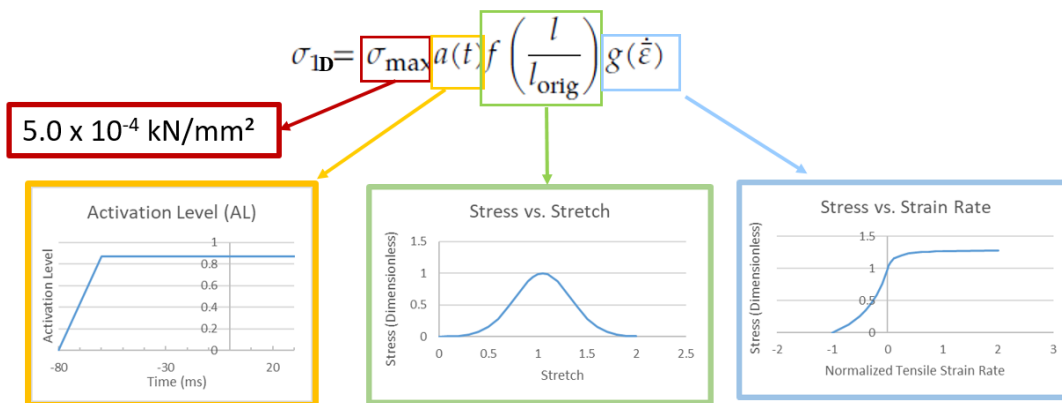
4 The helmet model consists of 182284 elements total.

Component	Material	Element Type	Material Model	Visco-elastic?
Helmet Shell	Polycarbonate	Shell	Elastic (*MAT_001)	No
Face Mask	Steel/Polyethylene	Beam	Elastic (*MAT_001)	No
Liner	Thermoplastic Polyurethane (Two types)	Shell	Hyperelastic rubber (*MAT_181)	Yes
Straps	Polyurethane/Nylon	Shell	Elastic (*MAT_001)	No
Comfort Pad	Polyurethane Foam (Soft, medium, firm)	Solid	Fu-Chang Foam (*MAT_181)	Yes

1 **Table S4 Helmet Modelling Details**

2 **Description of Muscle Implementation in the HBM**

3 The force in the 1D active muscle elements is a function of three curves: (1)
 4 elongation of the element, (2) the rate of loading, and (3) the Activation Level (AL),
 5 which is a function of time (Figure). The default values of these three curves are shown
 6 in Figure S1. The default AL curve represents a startle response, with a 74 ms delay prior
 7 to impact. The muscle elements are held in place by 1D elements that are fixed to the
 8 vertebrae.



9

10 **Figure S2 1D Muscle Element Inputs**

1 The muscles in the GHBMC-HBM are classified as flexor muscles and extensor
 2 muscles (Table S5). The AL curve is scaled by a certain factor for the flexor muscles and
 3 by a different value for the extensor muscles. All flexor muscles are assigned the same
 4 AL, and all the extensor muscles are assigned the same AL.

5 The classification of each muscle in the neck is shown in Table S5. The extensor
 6 muscles tend to rotate the head backwards, and the flexor muscles tend to rotate the
 7 head forwards.



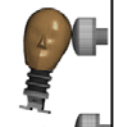

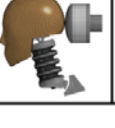





Muscle	Function	Muscle	Function
Anterior Scalene	Flexor	Multifidus	Extensor
Middle Scalene		Semispinalis Capitis	
Posterior Scalene		Semispinalis Cervicis	
Rectus Capitis Anterior		Longissimus Capitis	
Rectus Capitis Lateral		Longissimus Cervicis	
Omohyoid		Iliocostalis	
Sternocleidomastoid		Splenius Capsitis	
Longus Capitus		Splenius Cervicis	
Longus Colli		Levator Scapula	
Sternohyoid		Oblique Capitis Inferior	
Sternothyroid		Oblique Capitis Superior	
Thyrohyoid		Rectus Capitis Posterior Major	
Mylohyoid		Rectus Capitis Posterior Minor	
Stylohyoid		Minor Rhomboid	
Digastric		Trapezius	
Geniohyoid			

8
 9 **Table S5 Summary of neck muscles included in model and extensor/flexor classification**

10 **Verification of the ATD Response against Experiment**

11 The ATD was verified against the available experimental data [7,28] (Figure S3)
 12 with the boundary conditions of the current study, with the CORA parameters outlined in

1 the current study, and similar CORA ratings were obtained to those in previous studies
 2 [27,28]. Additionally, lower neck moment (at the neck mount, or T1), head z acceleration
 3 and T1 acceleration were compared with the experiments, which were not previously
 4 used for helmet validation [27,28].

Bare Head Verification	3x Orientations	1x Impact Velocity	Helmeted Verification	3x Orientations	3x Impact Velocities
ATD Simulation  ATD Experiment 	Lateral  Frontal  Rear 	5.5 m/s	ATD Simulation  ATD Experiment 	Lateral  Frontal  Rear 	5.5 m/s 7.4 m/s 9.3 m/s

5

6 **Figure S3 Verification cases (3x Bare Head, 9x Helmeted).** Note that there were three repeat
 7 experiments completed for the bare head cases, and no repeats for the helmeted cases.

8 The results from the model verification (Table S6, Table S7) were similar to those
 9 found during model development [27,28]. The average CORA rating for the Bare-Head
 10 simulation and experiment was 0.79, which represents a good agreement between the
 11 simulation and experiment. Overall, the primary axis head kinematics (Linear acceleration
 12 and Angular velocity) were the most accurately predicted metrics by the model.

13

Row Labels	Acc. X	Acc. Y	Acc. Z	Ang. Vel. X	Ang. Vel. Y	Acc. T1	Mres T1	Acc. Ram	Fres Ram	Overall Average
Lateral										
5.5 m/s	-	0.83	0.72	0.93	-	0.73	0.71	0.74	0.79	0.78
Repeat 1	-	0.82	0.71	0.93	-	0.75	0.71	0.74	0.79	0.78

Repeat 2	-	0.84	0.73	0.93	-	0.73	0.72	0.75	0.80	0.78
Repeat 3	-	0.82	0.71	0.93	-	0.70	0.71	0.74	0.79	0.77
Frontal										
5.5 m/s	0.85	-	0.49	-	0.75	0.78	-	0.86	0.72	0.74
Repeat 1	0.85	-	0.47	-	0.75	0.81	-	0.88	0.72	0.74
Repeat 2	0.87	-	0.55	-	0.78	0.77	-	0.87	0.73	0.76
Repeat 3	0.83	-	0.47	-	0.73	0.78	-	0.82	0.70	0.72
Rear										
5.5 m/s	0.88	-	0.78	-	0.97	0.86	0.81	0.82	0.81	0.85
Repeat 1	0.90	-	0.79	-	0.96	0.83	0.82	0.82	0.83	0.85
Repeat 2	0.85	-	0.75	-	0.98	0.84	0.78	0.80	0.78	0.82
Repeat 3	0.88	-	0.80	-	0.98	0.92	0.82	0.84	0.81	0.86
Avg.	0.87	0.83	0.66	0.93	0.86	0.79	0.76	0.81	0.77	0.79

1 **Table S6 CORA ratings between bare head ATD simulations and experiments**

2 The average CORA rating for the helmeted simulation and experiment was 0.82,
3 which was slightly better than the bare head rating. In general, the higher speed impacts
4 had a better correlation with the experiment, which was preferable because the impact
5 speed of 9.3 m/s is associated with concussive impacts, while the low speed impact
6 represented a normal hit during gameplay. The rear and side impact cases showed a
7 better correlation than the frontal impact condition.

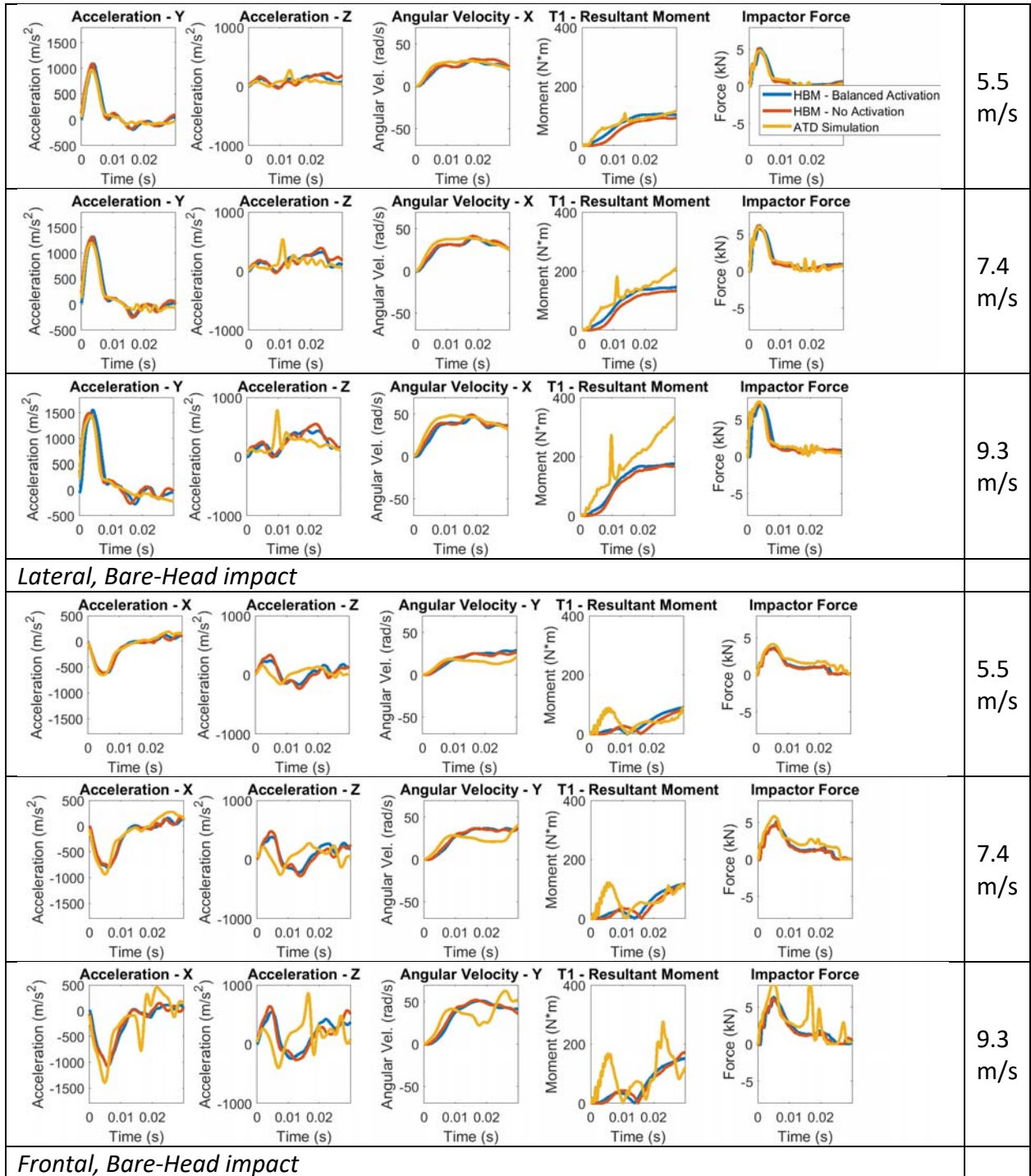
	Acc. X	Acc. Y	Acc. Z	Ang. Vel. X	Ang. Vel. Y	Acc. T1	Mres T1	Acc. Ram	Fres Ram	Overall Average
Lateral	-	0.96	0.74	0.91		0.92	0.83	0.90	0.88	0.88
5.5 m/s	-	0.95	0.56	0.91		0.90	0.78	0.85	0.89	0.83
7.4 m/s	-	0.97	0.79	0.91		0.94	0.85	0.95	0.87	0.90
9.3 m/s	-	0.95	0.86	0.91		0.92	0.85	0.91	0.89	0.90
Frontal	0.77	-	0.51	-	0.74	0.75	-	0.77	0.85	0.73
5.5 m/s	0.74	-	0.39	-	0.60	0.69	-	0.58	0.81	0.64
7.4 m/s	0.75	-	0.54	-	0.77	0.80	-	0.88	0.87	0.77
9.3 m/s	0.81	-	0.59	-	0.86	0.74	-	0.86	0.85	0.79
Rear	0.86	-	0.70	-	0.87	0.93	-	0.88	0.84	0.83
5.5 m/s	0.79	-	0.64	-	0.85	0.90	0.70	0.80	0.79	0.78
7.4 m/s	0.88	-	0.69	-	0.84	0.96	0.73	0.88	0.82	0.83

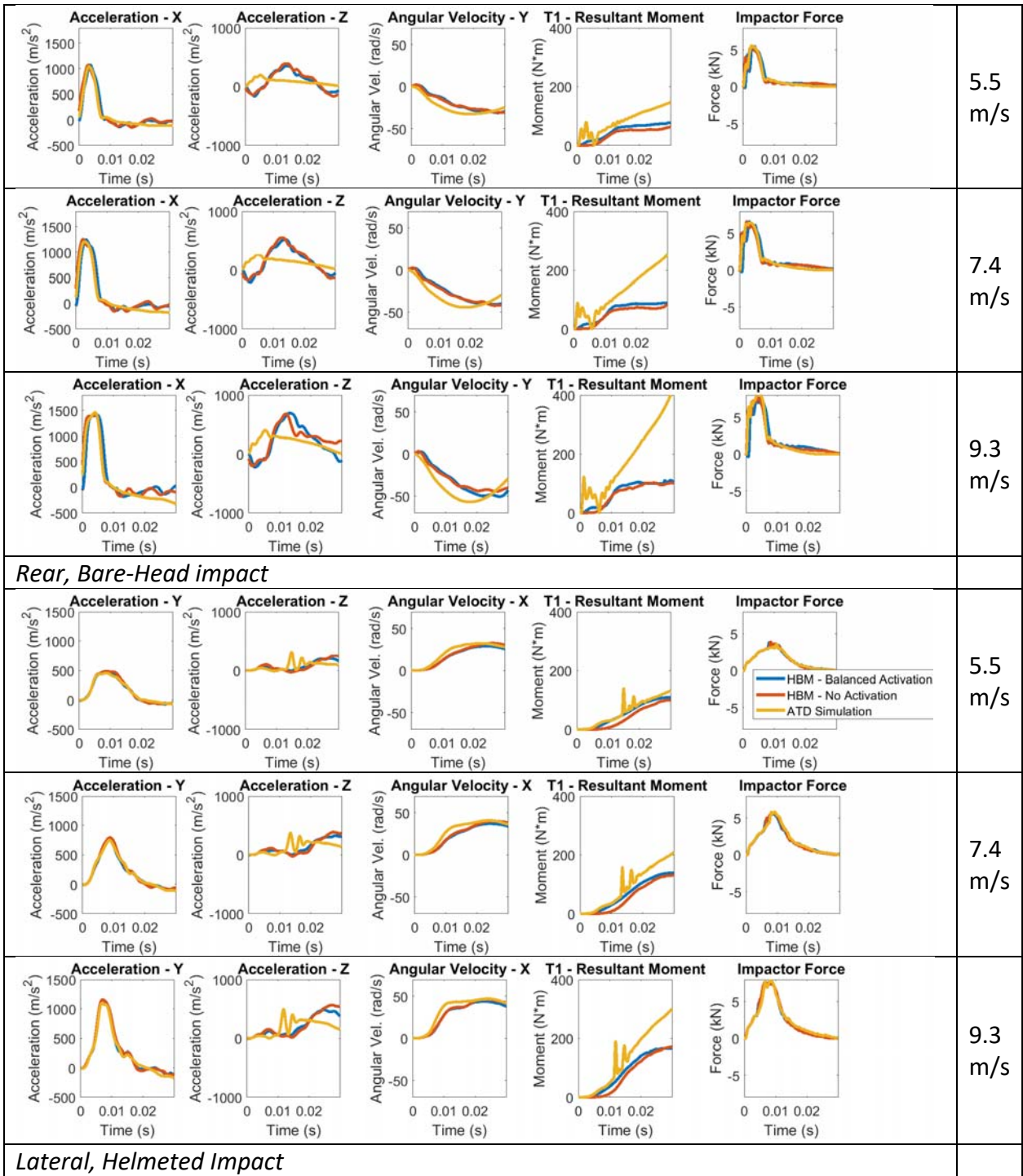
9.3 m/s	0.92	-	0.76	-	0.91	0.93	0.82	0.97	0.91	0.89
Avg.	0.82	0.96	0.65	0.91	0.80	0.86	0.79	0.85	0.86	0.82

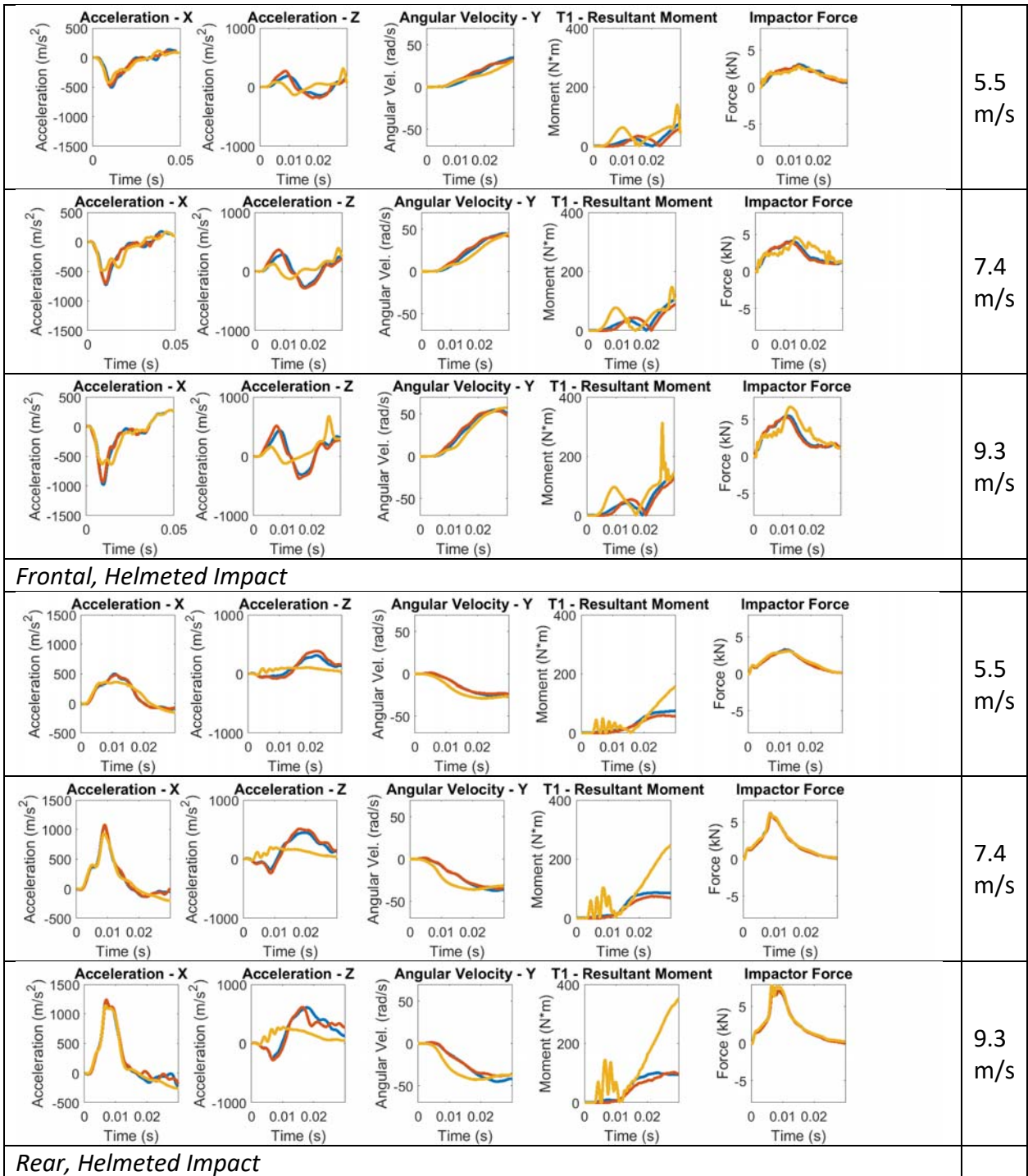
1 **Table S7 CORA ratings between helmeted ATD simulations and experiments**

2

1 Head kinematics in all Impacts







- 1
- 2
- 3
- 4

Figure S5 Bare Head and Helmeted Impact Kinematics, all velocities

Out of Plane Kinematics

1 Kinematics in the primary plane of motion (global Y-Z for lateral orientation, global X-Z
 2 for frontal and rear) were examined in the current study. The orientations used in the
 3 current study were chosen to minimize out-of-plane motion, to exercise the neck
 4 primarily in bending and axial compression. The 6 DOF kinematics are shown for the
 5 helmeted cases at 5.5 m/s, showing close to zero out-of-plane motion in the rear and
 6 frontal impacts, and small out of plane motions in the lateral impact (Figure S5, Figure
 7 S6).

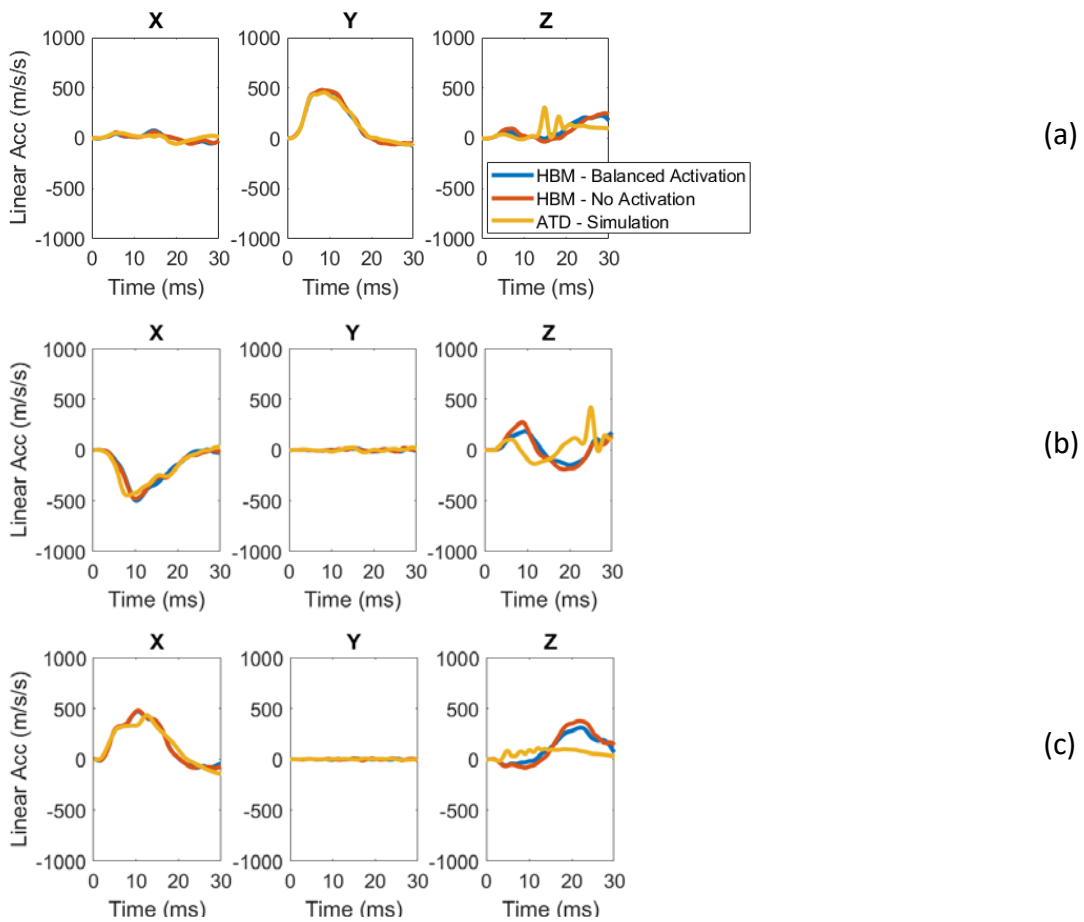


Figure S6 Helmeted Impact, 3DOF Linear Acceleration, 5.5 m/s, (a) Lateral, (b) Frontal, (c) Rear

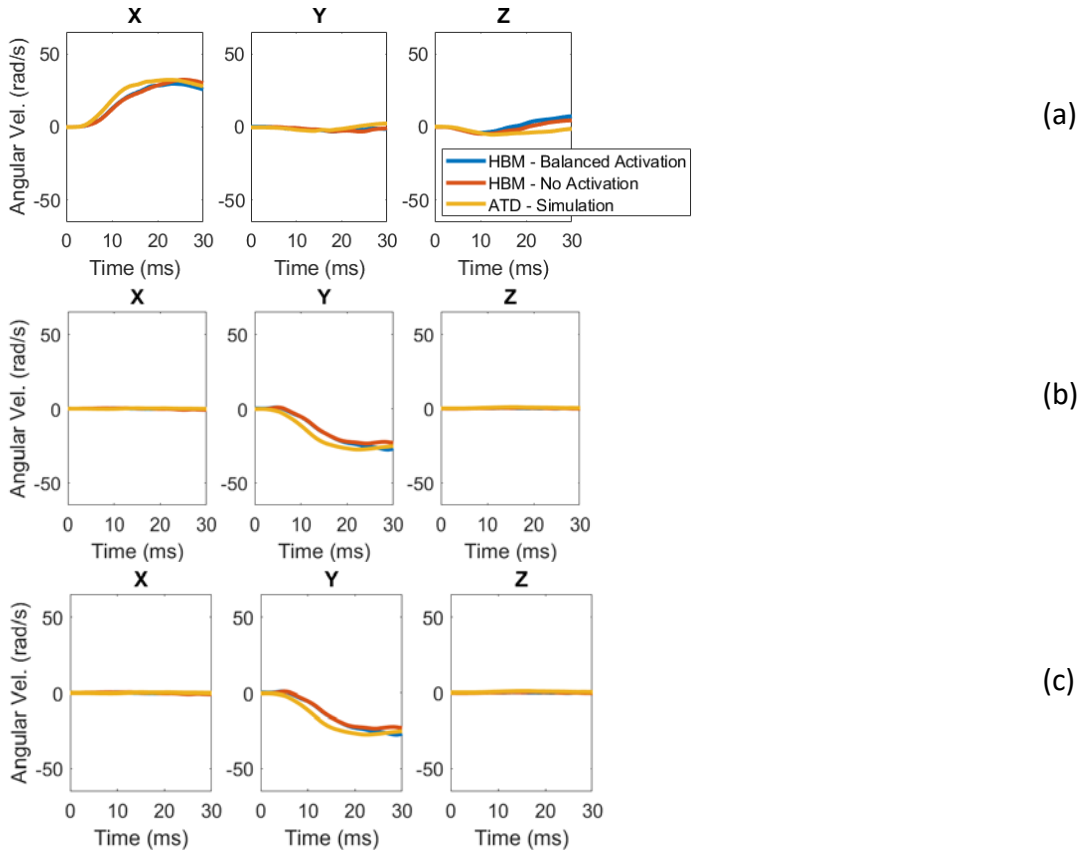


Figure S7 Helmeted Impact, 3DOF Angular Velocity, 5.5 m/s, (a) Lateral, (b) Frontal, (c) Rear

1